Supporting Information for:

Selective formation of spiroborate-based double-stranded *hetero*-helicates assisted by donor-acceptor interactions

Daisuke Taura,* Xiang Wang,† Masaki Ito and Eiji Yashima*

Department of Molecular and Macromolecular Chemistry, Graduate School of Engineering, Nagoya University, Chikusa-ku, Nagoya 464-8603, Japan.

† Present Address: Institute of Molecular Medicine (IMM), Shanghai Key Laboratory for Nucleic Acid Chemistry and Nanomedicine, Renji Hospital, School of Medicine, Shanghai Jiao Tong University, Shanghai 200240, China.

E-mail: taura@chembio.nagoya-u.ac.jp, yashima@chembio.nagoya-u.ac.jp

Table of Contents

1. Instruments and Materials.

Instruments

The melting points were measured on a Yanaco MP-500D micromelting point apparatus (Yanako, Kyoto, Japan) and were uncorrected. The IR spectra were recorded on a JASCO FT/IR-680 spectrophotometer (JASCO, Tokyo, Japan). The NMR spectra were measured using a Bruker Ascend 500 (Bruker Biospin, Billerica, MA, USA) spectrometer, a Varian 500AS (Agilent Technologies, Santa Clara, CA, USA) spectrometer or an Avance III HD 600 (Bruker, Billerica, MA, USA) spectrometer equipped with a cryoprobe operating at 500 MHz for ^{1}H and 126 MHz for ^{13}C (Bruker Ascend 500 and Varian 500AS) or 600 MHz for ^{1}H and 151 MHz for ^{13}C (Avance III HD 600) using tetramethylsilane (TMS) or a solvent residual peak as the internal standard. The absorption and CD spectra were measured in a 1-cm quartz cell using a JASCO V-570 spectrophotometer and a JASCO J-1500 spectropolarimeter, respectively. The temperature was controlled with a JASCO ETC-505 apparatus. The electrospray ionization (ESI) mass spectra were recorded using a JEOL JMS-T100CS mass spectrometer (JEOL, Akishima, Japan), a Thermo Fisher Scientific Exactive Plus mass spectrometer (Thermo Fisher Scientific, Waltham, MA, USA) or a Bruker Daltonics micrOTOF-QII mass spectrometer (Bruker Daltonics, Billerica, MA, USA). The recycling preparative HPLC was performed with an LC-908W-C60 liquid chromatograph (Japan Analytical Industry, Tokyo, Japan) equipped with two SEC columns (JAIGEL-1H (4 × 60 cm) and JAIGEL-2H (4 × 60 cm)) in series and a UV-visible detector (254 nm, JAI UV-3702), and $CHCl_3$ was used as the eluent. The chiral HPLC analyses were performed on a JASCO PU-4185 liquid chromatograph equipped with UV-visible (JASCO UV-2070 and JASCO MD-4010) and CD (JASCO CD-2095) detectors using a CHIRALPAK IA or a CHIRALPAK IB column (0.46 (i.d.) × 25 cm, Daicel, Osaka, Japan).

Materials

All starting materials were purchased from commercial suppliers and were used without further purification unless otherwise noted. Silica gel (SiO_2) for the flash chromatography was purchased from Kanto Chemical (Tokyo, Japan). **5**, **L2** and *homo*-**DH2**$_{Na2}$ were synthesized by the procedures reported previously.[S1]

2. Synthetic Procedures.

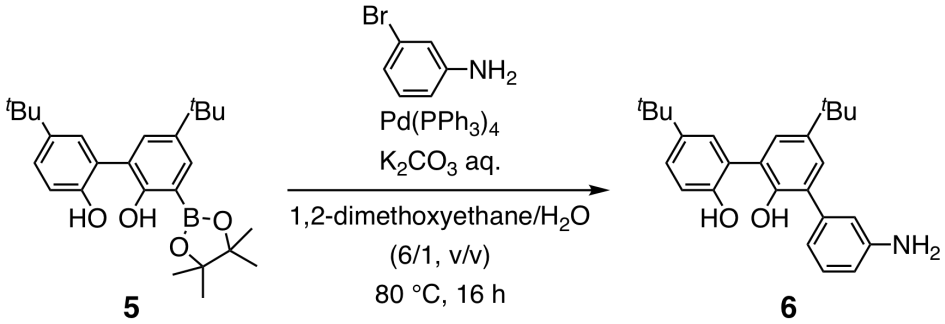

Scheme S1. Synthesis of compound **6**.

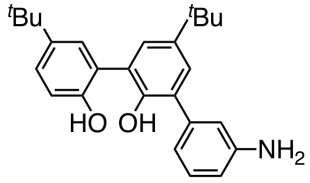

6. To a degassed solution of **5**[S1] (1.32 g, 3.11 mmol), 3-bromoaniline (0.50 g, 2.9 mmol) and K_2CO_3 (1.03 g, 7.45 mmol) in 1,2-dimethoxyethane (60 mL) and H_2O (10 mL) was added $Pd(PPh_3)_4$ (72 mg, 0.062 mmol), and the mixture was stirred at 80 °C for 16 h under nitrogen. After being cooled to room temperature, $CHCl_3$ (600 mL) was added to this. The solution was washed with brine (100 mL × 3) and dried over anhydrous Na_2SO_4. After filtration, the solvents were evaporated under reduced pressure and the residue was purified by flash chromatography (SiO_2, $CHCl_3$/MeOH = 1/0 to 9/1, v/v) and recycling preparative HPLC ($CHCl_3$) to afford **6** (0.76 g, 69% yield) as a brown solid. Mp: 92.5–93.7 °C. IR (KBr, cm^{-1}): 3379, 2961, 1617, 1610, 1229. ^1H NMR (500 MHz, $CDCl_3$, 25 °C): δ 7.35 (dd, J = 8.5, 2.5 Hz, 1H, ArH), 7.33–7.32 (m, 2H, ArH), 7.31–7.27 (m, 2H, ArH), 6.83–6.82 (m, 1H, ArH), 5.88 (br s, 1H, OH), 5.76 (br s, 1H, OH), 3.81 (br s, 2H, NH_2), 1.36 (s, 9H, *t*-Bu), 1.34 (s, 9H, *t*-Bu). ^{13}C NMR (126 MHz, $CDCl_3$, 23 °C): δ 151.27, 147.03, 146.82, 144.30, 144.01, 138.74, 130.30, 128.68, 128.42, 128.31, 127.28, 126.59, 125.12, 124.78, 119.55, 116.92, 116.08, 114.92, 34.46, 34.33, 31.70, 31.68. HRMS (ESI–): *m*/*z* calcd for $C_{26}H_{31}NO_2$ ($M–H^+$), 388.2277; found, 388.2285.

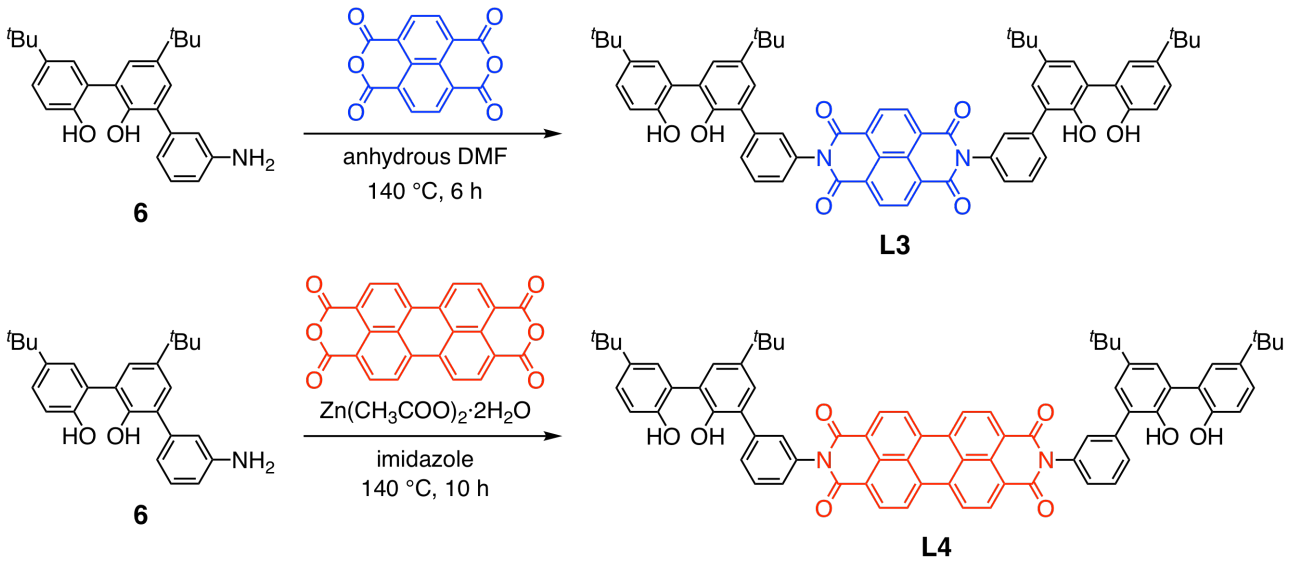

Scheme S2. Synthesis of ligands (**L2** and **L3**).

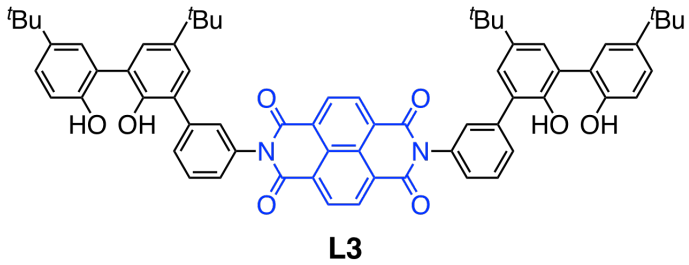

L3. A solution of **6** (180 mg, 0.462 mmol) and 1,4,5,8-naphthalenetetracarboxylic dianhydride (56 mg, 0.21 mmol) in anhydrous DMF (10 mL) was stirred at 140 °C for 6 h under nitrogen. After being cooled to room temperature, the solvent was evaporated under reduced pressure. The residue was purified by recycling preparative HPLC ($CHCl_3$) to afford **L3** (90 mg, 43% yield) as a brown solid. Mp: 209.3–210.5 °C. IR (KBr, cm^{-1}): 2961, 1716, 1677, 1580, 1346, 1251. ^1H NMR (500 MHz, $CDCl_3$, 50 °C): δ 8.86 (s, 4H, ArH), 7.75–7.69 (m, 4H, ArH), 7.602–7.596 (m, 2H, ArH), 7.44 (d, J = 2.5 Hz, 2H, ArH), 7.39–7.37 (m, 2H, ArH), 7.36 (dd, J = 8.5, 2.5 Hz, 2H, ArH), 7.31 (d, J = 2.5 Hz, 2H, ArH), 7.29 (d, J = 2.5 Hz, 2H, ArH), 6.99 (d, J = 8.5 Hz, 2H, ArH), 5.74 (s, 2H, OH), 5.53 (s, 2H, OH), 1.36 (s, 18H, *t*-Bu), 1.33 (s, 18H, *t*-Bu). ^{13}C NMR (126 MHz, $CDCl_3$, 26 °C): δ 163.08, 151.16, 147.47, 144.49, 144.26, 139.66, 134.71, 131.66, 130.40, 130.08, 129.80, 128.47, 128.16, 127.88, 127.65, 127.57, 127.30, 127.12, 126.97, 124.76, 124.00, 116.63, 34.51, 34.36, 31.70 (25 signals out of 26 expected ones due to the overlap of the CH_3 carbons of the two *t*-Bu groups). HRMS (ESI–): m/z calcd for $C_{66}H_{62}N_2O_8$ ($M–H^+$), 1009.4428; found, 1009.4448.

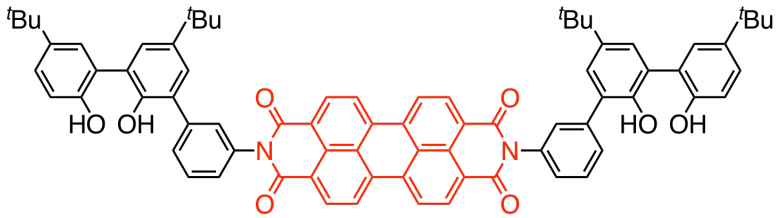

L4

L4. A mixture of **6** (360 mg, 0.924 mmol), perylene-3,4,9,10-tetracarboxylic dianhydride (181 mg, 0.461 mmol) and $Zn(CH_3COO)_2 \cdot 2H_2O$ (13.2 mg, 0.0601 mmol) in imidazole (4.0 g, 0.059 mol) was stirred at 140 °C for 10 h under nitrogen. After being cooled to room temperature, $CHCl_3$ (300 mL) was added to this. The solution was washed with 2 M HCl (200 mL × 3) and dried over anhydrous Na_2SO_4. After filtration, the solvent was evaporated under reduced pressure and the residue was purified by precipitation with $CHCl_3$/MeOH (1/4, v/v) to afford **L4** (330 mg, 63.1% yield) as a brown solid. Mp: > 300 °C. IR (KBr, cm^{-1}): 2961, 1703, 1664, 1594, 1578, 1359, 1255. ^1H NMR (500 MHz, $CDCl_3$, 50 °C): δ 8.72 (d, J = 8.0 Hz, 4H, ArH), 8.60 (d, J = 8.0 Hz, 4H, ArH), 7.67–7.61 (m, 6H, ArH), 7.43 (d, J = 2.5 Hz, 2H, ArH), 7.38–7.36 (m, 2H, ArH), 7.33 (dd, J = 8.5, 2.5 Hz, 2H, ArH), 7.30 (d, J = 2.5 Hz, 2H, ArH), 7.29 (d, J = 2.5 Hz, 2H, ArH), 6.97 (d, J = 8.5 Hz, 2H, ArH), 5.76 (br s, 2H, OH), 5.59 (br s, 2H, OH), 1.36 (s, 18H, *t*-Bu), 1.33 (s, 18H, *t*-Bu). ^{13}C NMR (151 MHz, $CDCl_3$, 50 °C): δ 163.34, 151.40, 147.33, 144.52, 144.10, 139.51, 135.05, 134.50, 131.55, 130.12, 130.07, 129.95, 129.41, 128.62, 128.28, 128.18, 127.82, 126.58, 126.21, 125.60, 125.09, 123.56, 123.27, 117.00, 34.53, 34.38, 31.76 (27 signals out of 29 expected ones due to the overlap of an aromatic carbon and the CH_3 carbons of the two *t*-Bu groups). HRMS (ESI–): *m*/*z* calcd for $C_{76}H_{66}N_2O_8$ ($M–H^+$), 1133.4741; found, 1133.4707.

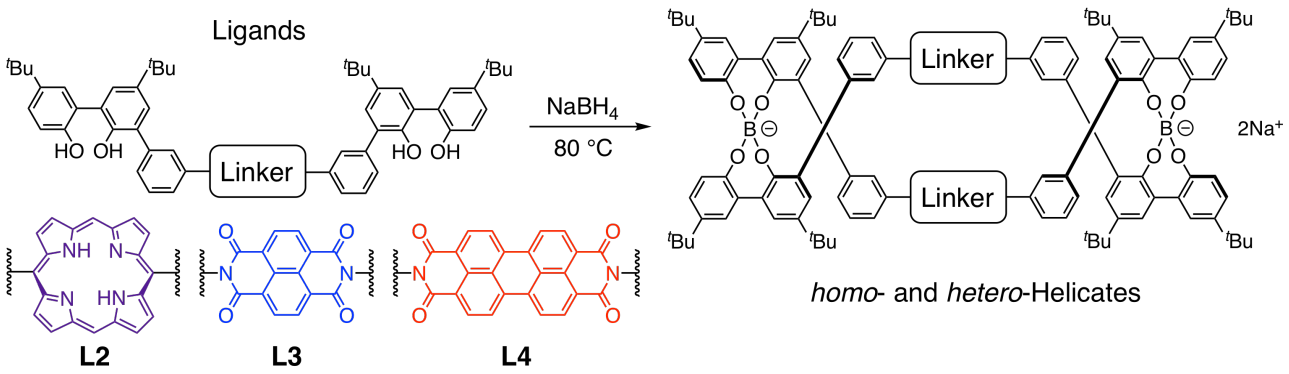

Scheme S3. Synthesis of *homo*- and *hetero*-helicates.

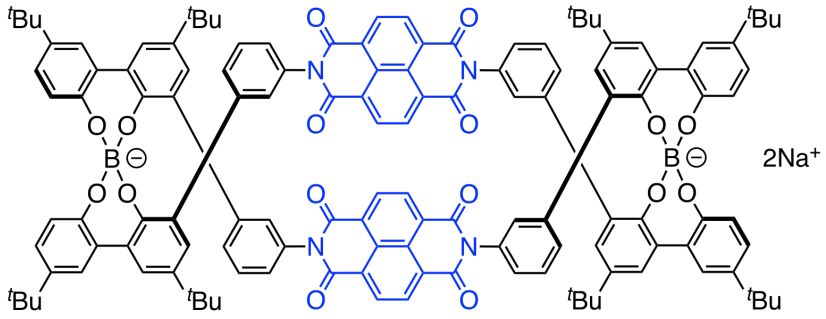

homo-**DH3**$_{Na2}$

***homo*-DH3$_{Na2}$.** To a solution of **L3** (27.1 mg, 26.8 μmol) in anhydrous 1,2-dichloroethane (10.6 mL) was added a solution of $NaBH_4$ in EtOH (75 mM, 0.53 mL, 40 μmol) under nitrogen. After stirring at 80 °C for 9 h, the mixture was cooled to room temperature and the solvents were evaporated under reduced pressure. The residue was washed with *n*-hexane to quantitatively afford *homo*-**DH3**$_{Na2}$ as a dark brown solid. Mp: > 300 °C. IR (KBr, cm^{-1}): 2960, 1718, 1678, 1579, 1346, 1251, 1001. ^1H NMR (500 MHz, CD_3CN, 25 °C): δ 8.44 (s, 8H, ArH), 7.72–7.69 (m, 4H, ArH), 7.43 (d, J = 2.5 Hz, 4H, ArH), 7.40 (d, J = 2.5 Hz, 4H, ArH), 7.27 (dd, J = 8.5, 2.5 Hz, 4H, ArH), 7.212–7.207 (m, 8H, ArH), 6.95–6.89 (m, 8H, ArH), 6.77 (d, J = 8.5 Hz, 4H, ArH), 1.49 (s, 36H, *t*-Bu), 1.40 (s, 36H, *t*-Bu). ^{13}C NMR (151 MHz, CD_3CN, 25 °C): δ 163.42, 156.12, 153.23, 143.13, 143.10, 142.49, 135.03, 132.58, 132.50, 132.14, 131.61, 130.09, 127.91, 127.65, 127.36, 127.19, 126.92, 126.24, 125.90, 125.61, 122.08, 34.85, 34.75, 32.11, 32.01 (25 signals out of 26 expected ones due to the overlap of an aromatic carbon). HRMS (ESI–): *m*/*z* calcd for $C_{132}H_{116}B_2N_4Na_2O_{16}$ ($M–2Na^+$), 1017.4292; found, 1017.4303.

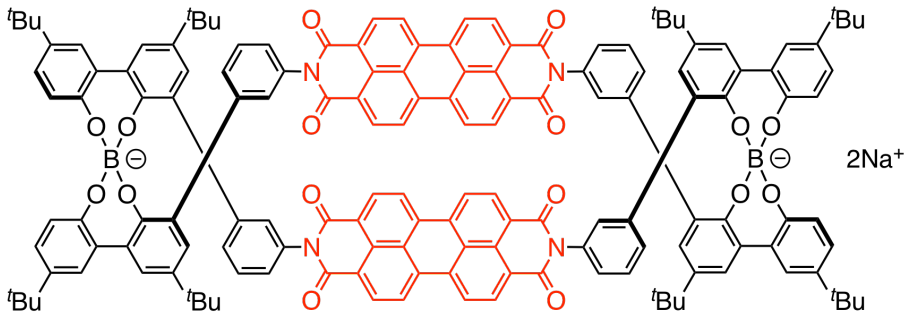

homo-**DH4**$_{Na2}$

***homo*-DH4$_{Na2}$.** A mixture of **L4** (57 mg, 50 μmol) and $NaBH_4$ (2.8 mg, 74 μmol) in anhydrous toluene (20 mL) and EtOH (1.0 mL) was stirred at 80 °C for 13 h under nitrogen. After being cooled to room temperature, the solvents were evaporated under reduced pressure. The residue was then purified by precipitation with THF/*n*-hexane (2/1, v/v) to afford *homo*-**DH4**$_{Na2}$ (23 mg, 40% yield) as a dark red solid. Mp: > 300 °C. IR (KBr, cm^{-1}): 2958, 1704, 1663, 1594, 1577, 1359, 1256, 1002. ^{1}H NMR (500 MHz, CD_3CN, 25 °C): δ 8.28 (br d, 4H, ArH), 8.05 (br d, 4H, ArH), 7.94 (br d, 4H, ArH), 7.85 (br d, 4H, ArH), 7.68–7.66 (m, 4H, ArH), 7.45 (d, J = 2.5 Hz, 4H, ArH), 7.43 (d, J = 2.5 Hz, 4H, ArH), 7.28–7.26 (m, 8H, ArH), 7.20 (d, J = 2.5 Hz, 4H, ArH), 6.95–6.89 (m, 8H, ArH), 6.76 (d, J = 8.5 Hz, 4H, ArH), 1.49 (s, 36H, *t*-Bu), 1.41 (s, 36H, *t*-Bu). ^{13}C NMR (151 MHz, CD_3CN, 27 °C): δ 163.80, 156.14, 153.24, 143.03, 142.98, 142.59, 135.51, 134.41, 134.01, 133.22, 132.62, 131.84, 131.67, 131.37, 130.79, 130.75, 130.12, 129.09, 127.78, 127.60, 127.32, 126.49, 125.76, 125.69, 125.63, 124.65, 124.29, 123.99, 123.40, 122.03, 34.89, 34.76, 32.20, 32.04. HRMS (ESI–): *m*/*z* calcd for $C_{152}H_{124}B_2N_4Na_2O_{16}$ ($M–2Na^+$), 1141.4605; found, 1141.4631.

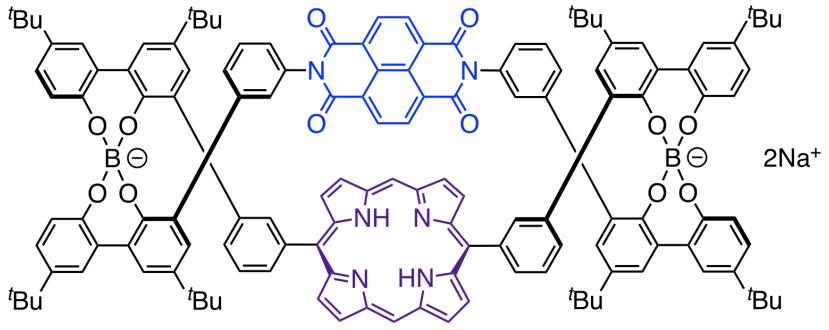

hetero-**DH2·3**$_{Na2}$

***hetero*-DH2·3$_{Na2}$.** A mixture of **L2**[S1] (26 mg, 25 μmol), **L3** (25 mg, 25 μmol) and $NaBH_4$ (2.8 mg, 74 μmol) in anhydrous 1,2-dichloroethane (20 mL) and EtOH (1.0 mL) was stirred at 80 °C for 13 h under nitrogen. After being cooled to room temperature, the solvents were evaporated under reduced pressure. The formation of the *hetero*-**DH2·3**$_{Na2}$ was investigated by measuring the ^{1}H NMR and negative-mode ESI mass spectra of the products (Fig. S5e). The product molar ratio of the *homo*-

DH2$_{\mathbf{Na2}}$[S1] : *hetero*-**DH2·3**$_{\mathbf{Na2}}$: *homo*-**DH3**$_{\mathbf{Na2}}$ was roughly estimated to be 6 : 93 : 1 from the ^{1}H NMR (run 3 in Table 1).

The formation of the *hetero*-**DH2·3**$_{\mathbf{Na2}}$ was also investigated using **L2**[S1] and **L3** at a different feed molar ratio ([**L2**[S1]]/[**L3**] = 1/1.5) (run 4 in Table 1).

***hetero*-DH2·3$_{\mathbf{Na2}}$.** A mixture of **L2**[S1] (26.4 mg, 25.0 μmol), **L3** (37.9 mg, 37.5 μmol) and $NaBH_4$ (2.8 mg, 74 μmol) in anhydrous 1,2-dichloroethane (20 mL) and EtOH (1.0 mL) was stirred at 80 °C for 11 h under nitrogen. After being cooled to room temperature, the solvents were evaporated under reduced pressure. The product molar ratio of the *homo*-**DH2**$_{\mathbf{Na2}}$[S1] : *hetero*-**DH2·3**$_{\mathbf{Na2}}$: *homo*-**DH3**$_{\mathbf{Na2}}$ was roughly estimated to be 1 : 98 : 1 on the basis of the ^{1}H NMR spectrum of the products. The residue was then purified by precipitation with THF/*n*-hexane (1/2, v/v) to afford *hetero*-**DH2·3**$_{\mathbf{Na2}}$ (12 mg, 23% yield) as a dark red solid. Mp: > 300 °C. IR (KBr, cm^{-1}): 2960, 1717, 1675, 1579, 1346, 1251, 999. ^{1}H NMR (500 MHz, CD_3CN, 25 °C): δ 10.23 (s, 2H, CH=C), 9.49 (d, J = 4.6 Hz, 2H, C*H*=CH), 9.19 (d, J = 4.6 Hz, 2H, CH=C*H*), 9.06–9.03 (m, 4H, C*H*=C*H*), 8.172–8.165 (m, 2H, ArH), 8.13–8.11 (m, 2H, ArH), 7.81–7.79 (m, 2H, ArH), 7.73 (d, J = 2.6 Hz, 2H, ArH), 7.71 (d, J = 2.6 Hz, 2H, ArH), 7.68–7.66 (m, 2H, ArH), 7.63 (d, J = 2.6 Hz, 2H, ArH), 7.51 (d, J = 2.6 Hz, 2H, ArH), 7.46 (d, J = 2.5 Hz, 2H, ArH), 7.45 (d, J = 2.5 Hz, 2H, ArH), 7.31 (t, J = 7.5 Hz, 2H, ArH), 7.29 (dd, J = 8.5, 2.6 Hz, 2H, ArH), 7.23 (dd, J = 8.5, 2.5 Hz, 2H, ArH), 6.88 (t, J = 8.0 Hz, 2H, ArH), 6.84 (br d, 2H, ArH), 6.80 (d, J = 8.5 Hz, 2H, ArH), 6.74 (d, J = 8.5 Hz, 2H, ArH), 6.66–6.45 (m, 2H, ArH), 6.37–6.35 (m, 2H, ArH), 6.33 (br d, 2H, ArH), 1.79 (s, 18H, *t*-Bu), 1.56 (s, 18H, *t*-Bu), 1.41 (s, 18H, *t*-Bu), 1.39 (s, 18H, *t*-Bu), –4.22 (s, 2H, NH). ^{13}C NMR (151 MHz, CD_3CN, 27 °C): δ161.90, 161.43, 156.23, 156.00, 153.62, 153.46, 143.33, 143.21, 143.09, 142.95, 142.76, 141.36, 140.30, 137.43, 134.62, 134.17, 133.78, 133.73, 133.45, 133.20, 133.09, 132.79, 132.63, 131.92, 131.88, 131.71, 131.32, 130.85, 130.38, 128.40, 128.17, 127.87, 127.76, 127.65, 127.33, 127.11, 126.50, 126.23, 126.07, 125.88, 125.82, 125.70, 124.29, 124.14, 123.86, 122.28, 122.10, 120.60, 105.97, 35.18, 34.99, 34.77, 34.74, 32.45, 32.15, 32.03, 32.01. HRMS (ESI–): m/z calcd for $C_{138}H_{124}B_2N_6Na_2O_{12}$ (M–2Na$^+$), 1039.4737; found, 1039.4718.

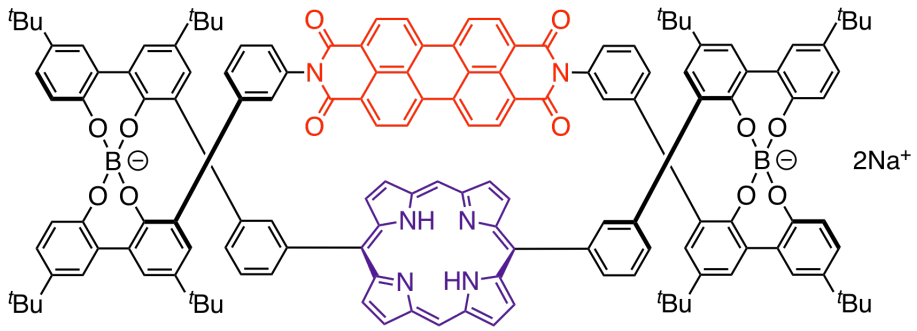

hetero-**DH2**·$\mathbf{4}_{Na2}$

***hetero*-DH2·$\mathbf{4}_{Na2}$.** To a solution of **L2**[S1] (2.6 mg, 2.5 μmol) and **L4** (2.8 mg, 2.5 μmol) in anhydrous 1,2-dichloroethane (2.0 mL) was added a solution of $NaBH_4$ in EtOH (75 mM, 0.10 mL, 7.5 μmol). After stirring at 80 °C for 9 h under nitrogen, the mixture was cooled to room temperature and the solvents were evaporated under reduced pressure. The formation of the *hetero*-**DH2**·$\mathbf{4}_{Na2}$ was investigated by measuring the ^{1}H NMR and negative-mode ESI mass spectra of the products (Figs. S7e and S8).

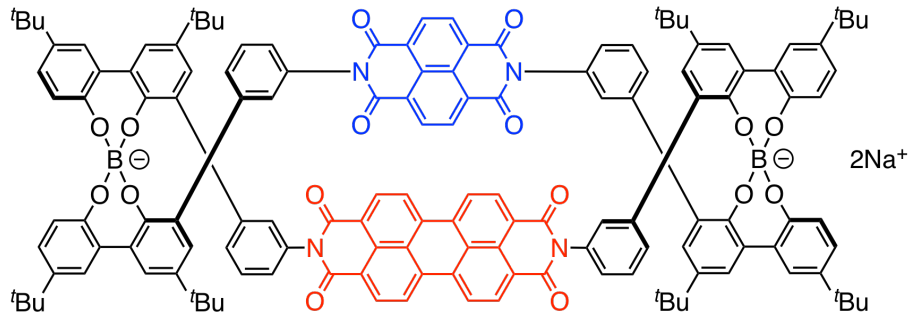

hetero-**DH3**·$\mathbf{4}_{Na2}$

***hetero*-DH3·$\mathbf{4}_{Na2}$.** To a solution of **L3** (5.1 mg, 5.0 μmol) and **L4** (5.7 mg, 5.0 μmol) in anhydrous 1,2-dichloroethane (4.0 mL) was added a solution of $NaBH_4$ in EtOH (75 mM, 0.20 mL, 15 μmol). After stirring at 80 °C for 9 h under nitrogen, the mixture was cooled to room temperature and the solvents were evaporated under reduced pressure. The residue was then washed with *n*-hexane. The formation of the *hetero*-**DH3**·$\mathbf{4}_{Na2}$ was investigated by measuring the ^{1}H NMR and negative-mode ESI mass spectra of the reaction products (Figs. S9e and S10).

3. ^{1}H NMR and ESI Mass Spectra of the *homo*- and *hetero*-Helicates.

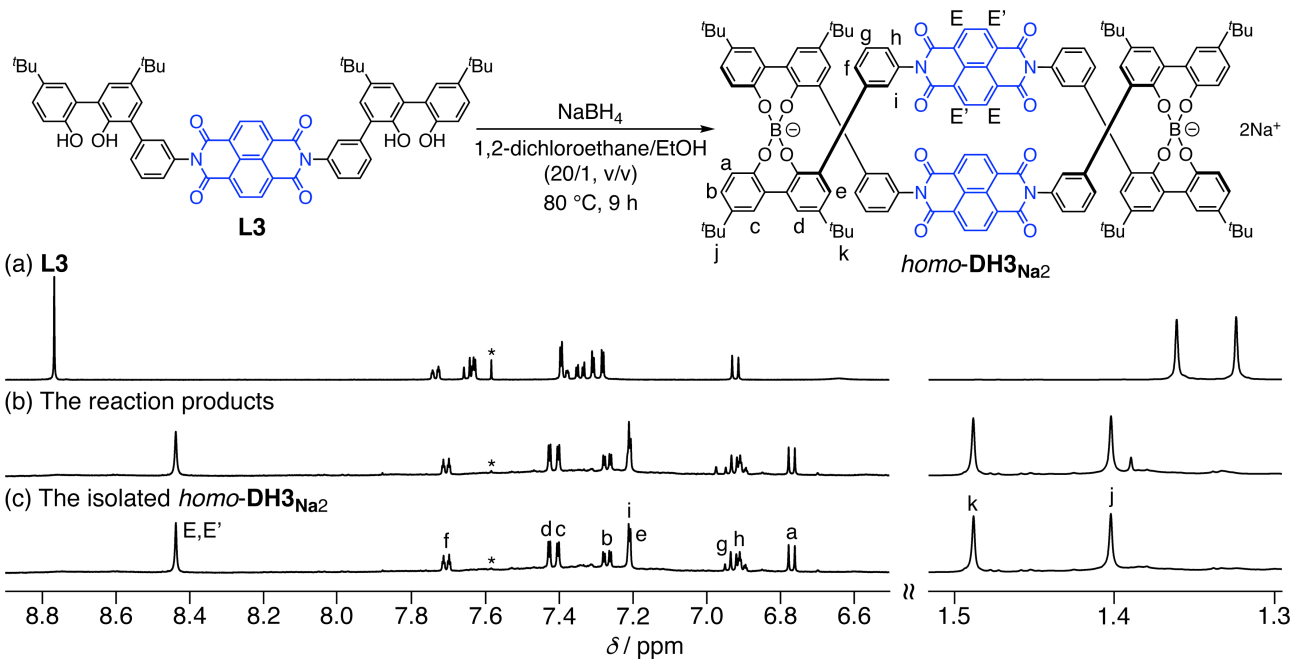

Fig. S1 Partial ^{1}H NMR spectra (500 MHz, CD_3CN, rt) of (a) **L3**, (b) the products after the reaction of **L3** with $NaBH_4$ (1.5 equiv) in 1,2-dichloroethane/EtOH (20/1, v/v) at 80 °C for 9 h and (c) the *homo*-**DH3**$_{Na2}$ isolated from the reaction products (b). The peak assignments of the isolated *homo*-**DH3**$_{Na2}$ were done on the basis of *g*COSY and ROESY spectra (Figs. S12 and S13). * denotes the proton from the residual $CHCl_3$ (a–c).

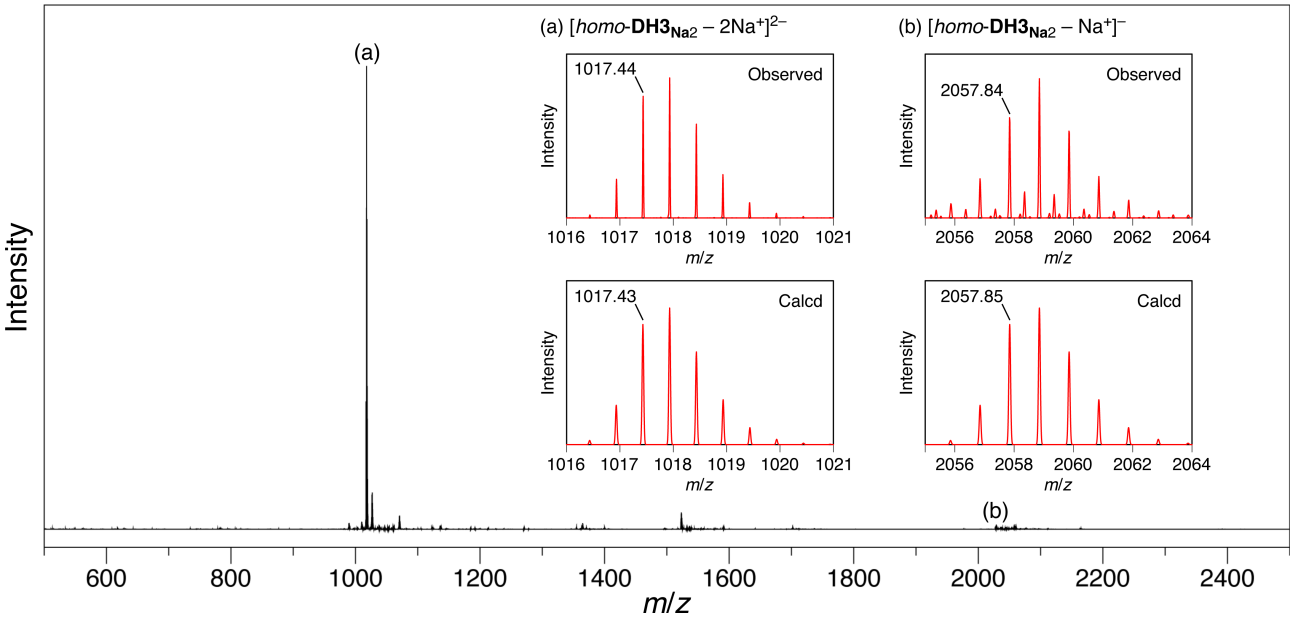

Fig. S2 Negative-mode ESI mass spectrum (CH_3CN/MeOH = 1/1, v/v) of the *homo*-**DH3**$_{Na2}$ isolated from the reaction products (Fig. S1c).

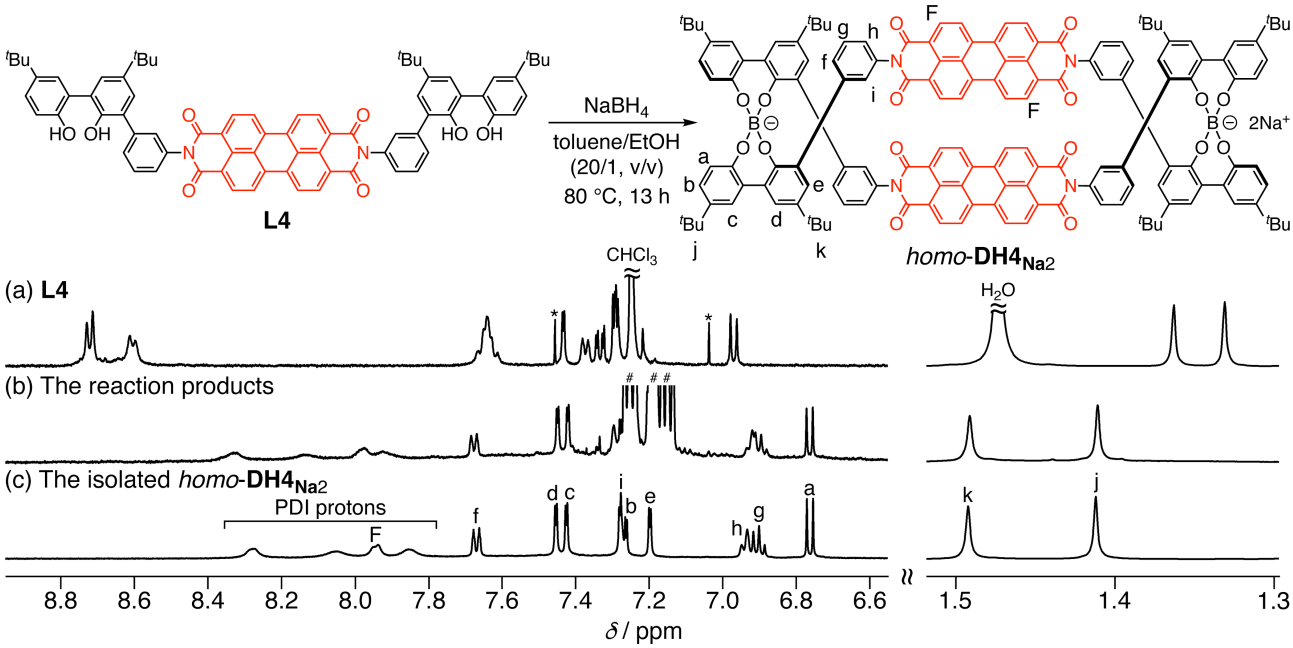

Fig. S3 Partial ^{1}H NMR spectra (500 MHz, rt) of (a) **L4**, (b) the products after the reaction of **L4** with $NaBH_4$ (1.5 equiv) in toluene/EtOH (20/1, v/v) at 80 °C for 13 h and (c) the *homo*-**DH4**$_{Na2}$ isolated from the reaction products (b) measured in $CDCl_3$ (a) and CD_3CN (b,c). * and # denote the ^{13}C satellite peaks (a) and the protons from the residual toluene used as the reaction solvent (b), respectively. The peak assignments of the isolated *homo*-**DH4**$_{Na2}$ were done on the basis of *g*COSY and ROESY spectra (Figs. S14 and S15). Because of poor solubility of **L4** in CD_3CN, $CDCl_3$ was used as the solvent.

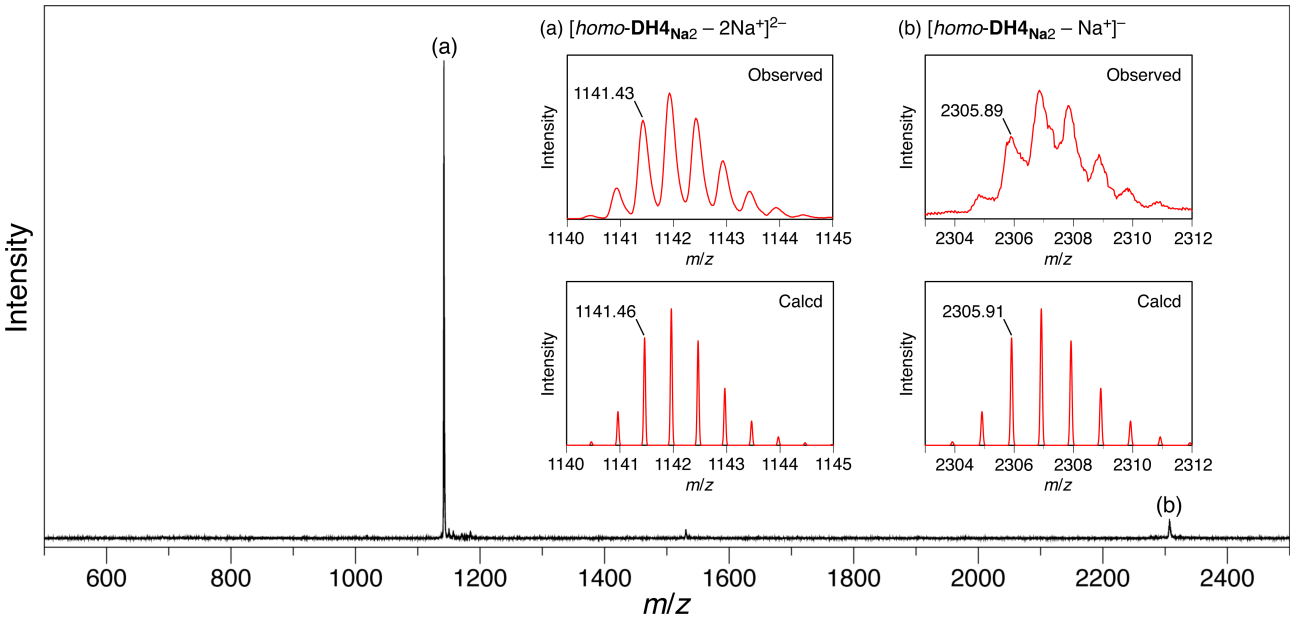

Fig. S4 Negative-mode ESI mass spectrum (CH_3CN/MeOH = 1/1, v/v) of the *homo*-**DH4**$_{Na2}$ isolated from the reaction products (Fig. S3c).

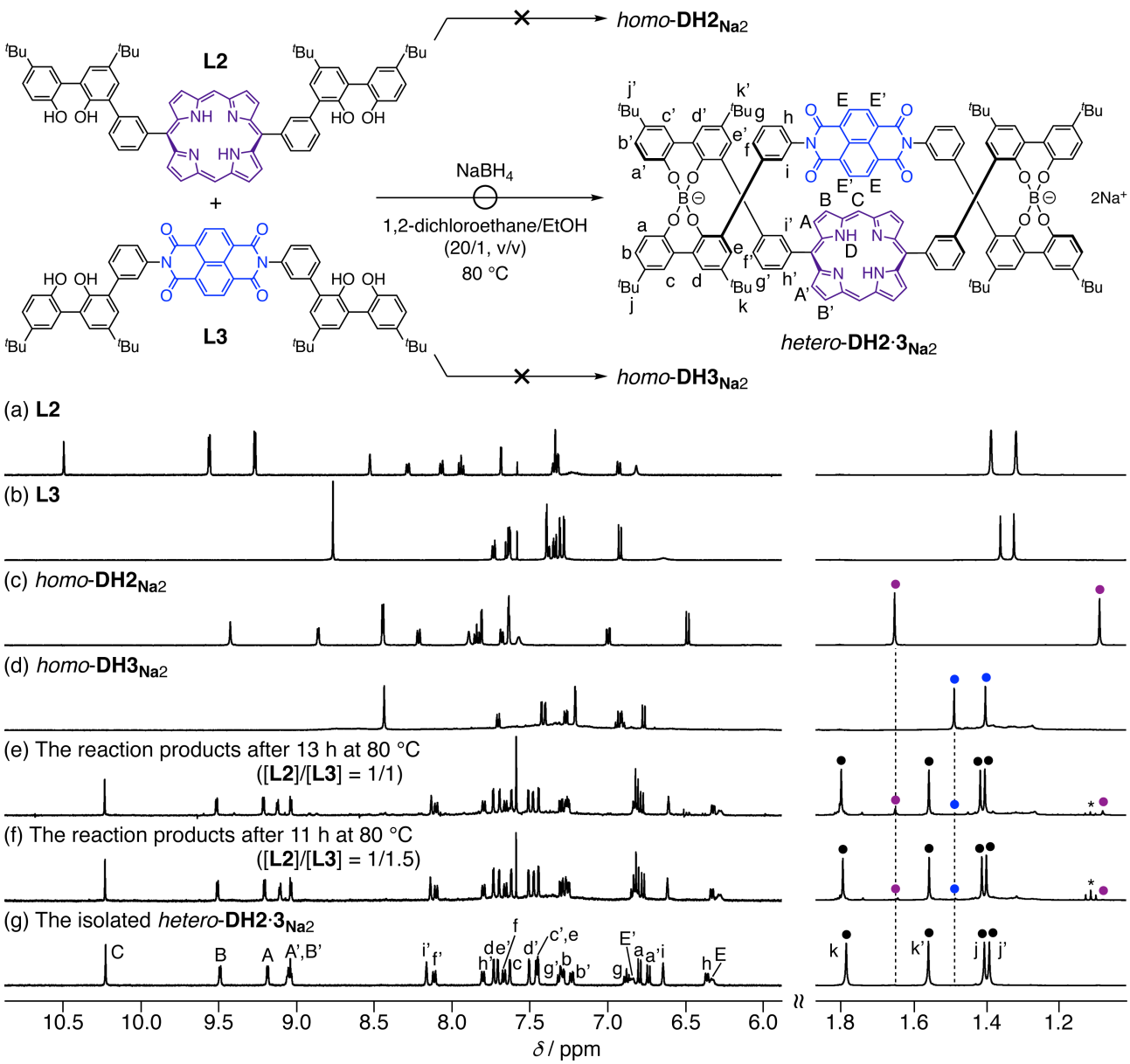

Fig. S5 Partial ^{1}H NMR spectra (500 MHz, CD_3CN, rt) of (a) **L2**,[S1] (b) **L3**, (c) *homo*-**DH2**$_{Na2}$,[S1] (d) *homo*-**DH3**$_{Na2}$, (e,f) the products after the reaction of **L2**[S1] and **L3** ([**L2**[S1]]/[**L3**] = 1/1 (e) and 1/1.5 (f)) with $NaBH_4$ (1.5 (e) and 1.2 equiv (f)) in 1,2-dichloroethane/EtOH (20/1, v/v) at 80 °C for 13 (e) and 11 h (f) and (g) the *hetero*-**DH2**·**3**$_{Na2}$ isolated from the reaction products (f). * denotes the protons from the residual EtOH used as the reaction solvent. The peak assignments of the isolated *hetero*-**DH2**·**3**$_{Na2}$ were done on the basis of *g*COSY and ROESY spectra (Figs. S16 and S17).

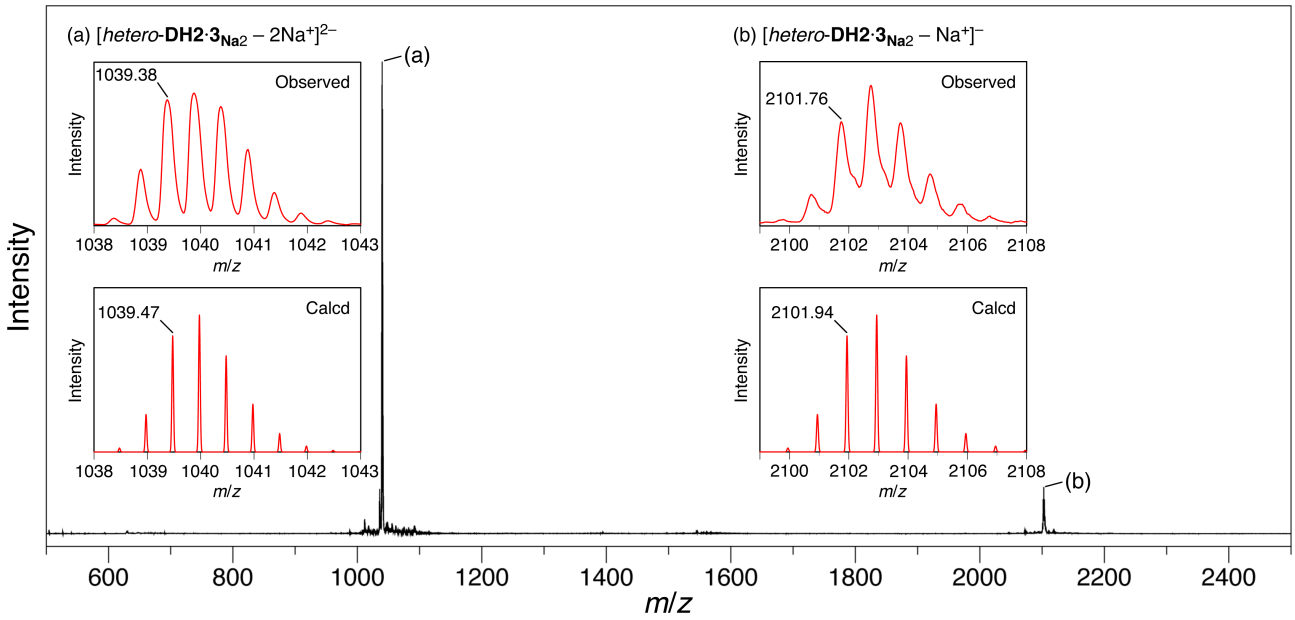

Fig. S6 Negative-mode ESI mass spectrum (CH_3CN/MeOH = 1/1, v/v) of the *hetero*-**DH2**·$\mathbf{3}_{Na2}$ isolated from the reaction products (Fig. S5g).

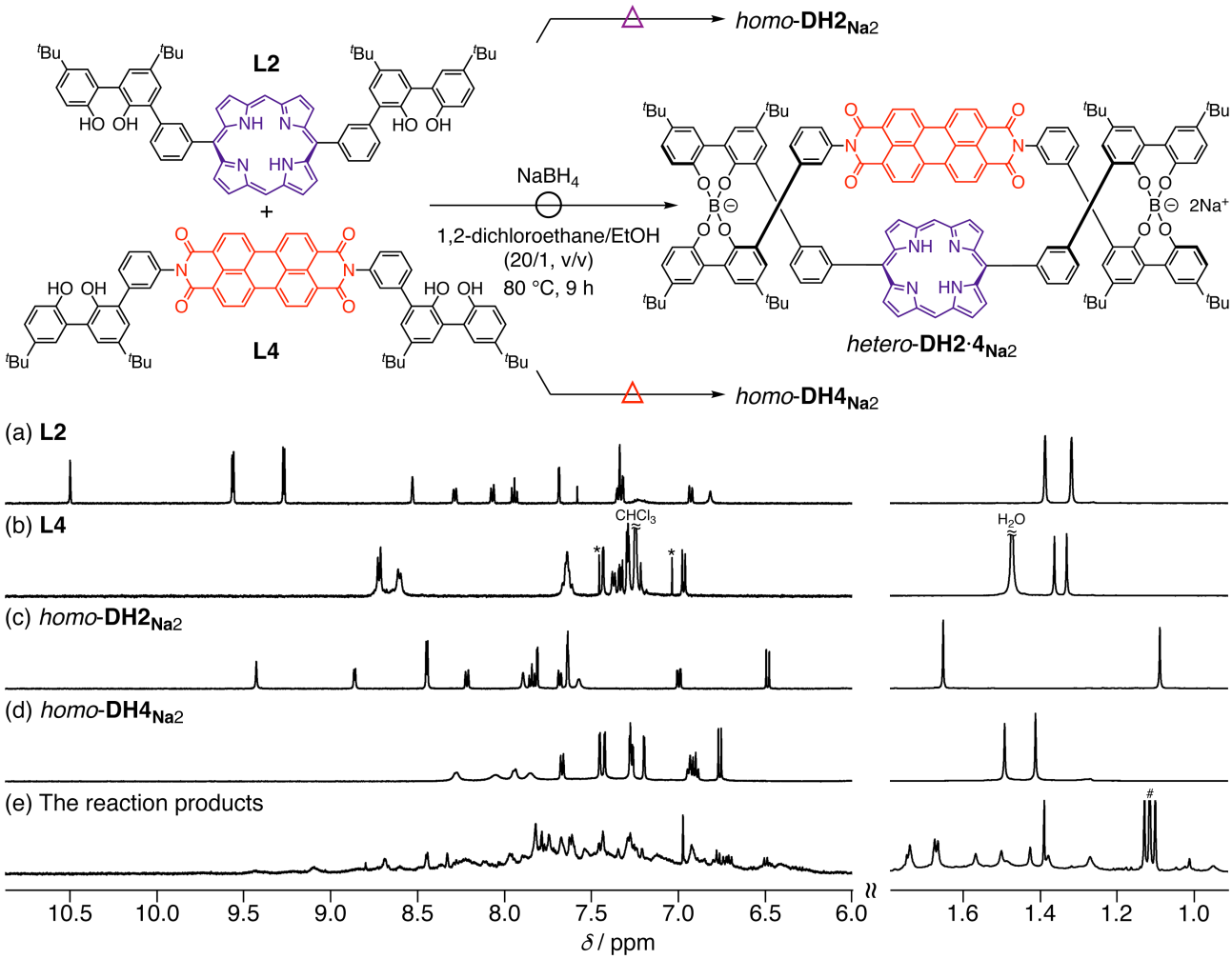

Fig. S7 Partial ^{1}H NMR spectra (500 MHz, rt) of (a) **L2**,[S1] (b) **L4**, (c) *homo*-**DH2**$_{Na2}$,[S1] (d) *homo*-**DH4**$_{Na2}$ and (e) the products after the reaction of **L2**[S1] and **L4** ([**L2**[S1]]/[**L4**] = 1/1) with $NaBH_4$ (1.5 equiv) in 1,2-dichloroethane/EtOH (20/1, v/v) at 80 °C for 9 h measured in CD_3CN (a,c–e) and $CDCl_3$ (b). * and # denote the ^{13}C satellite peaks of the solvent (b) and the protons from the residual EtOH used as the reaction solvent (e), respectively.

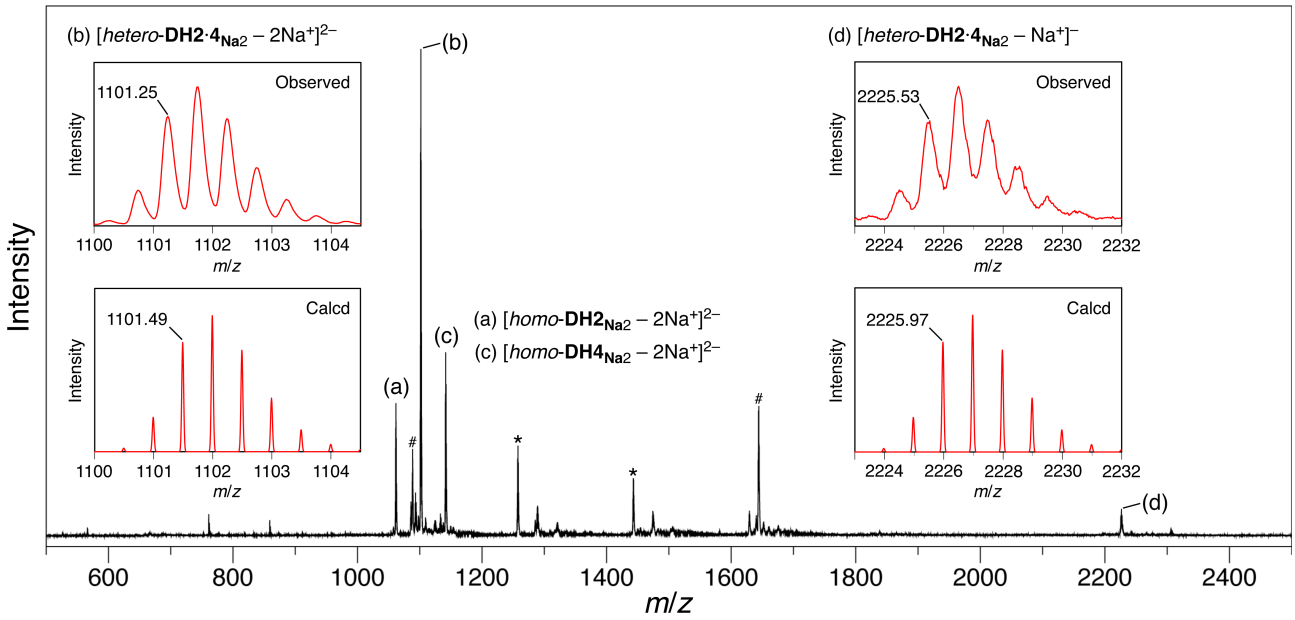

Fig. S8 Negative-mode ESI mass spectrum (CH_3CN/MeOH = 1/1, v/v) of the products after the reaction of $\mathbf{L2}^{S1}$ and **L4** ([$\mathbf{L2}^{S1}$]/[**L4**] = 1/1) with $NaBH_4$ (1.5 equiv) in 1,2-dichloroethane/EtOH (20/1, v/v) at 80 °C for 9 h (Fig. S7e). The divalent peaks (a) and (c) were assigned to the *homo*-helicates ([*homo*-$\mathbf{DH2}_{\mathbf{Na}2}{}^{S1}$ – $2Na^+]^{2-}$ (a) and [*homo*-$\mathbf{DH4}_{\mathbf{Na}2}$ – $2Na^+]^{2-}$ (c)), respectively. * and # denote the peaks for unknown products (*) and divalent and trivalent peaks for a trimeric macrocycle composed of two $\mathbf{L2}^{S1}$ and one **L4** ligands bridged by three spiroborates ([*macrocycle*-$\mathbf{2_2{\cdot}4}_{\mathbf{Na}3}$ – $Na^+]^{2-}$ and [*macrocycle*-$\mathbf{2_2{\cdot}4}_{\mathbf{Na}3}$ – $3Na^+]^{3-}$ (#), respectively.

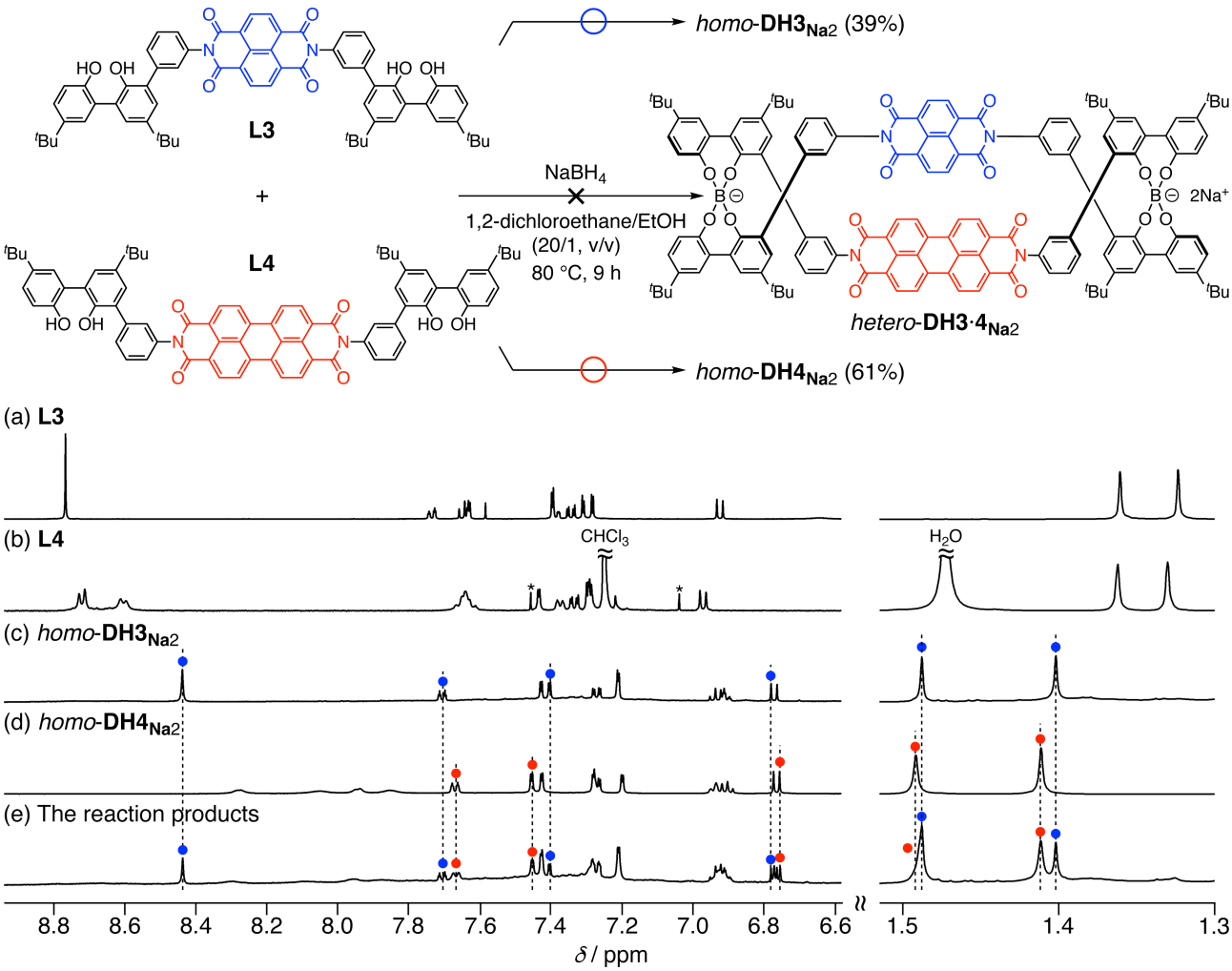

Fig. S9 Partial ^{1}H NMR spectra (500 MHz, CD_3CN, rt) of (a) **L3**, (b) **L4**, (c) *homo*-**DH3**$_{Na2}$, (d) *homo*-**DH4**$_{Na2}$ and (e) the products after the reaction of **L3** and **L4** ([**L3**]/[**L4**] = 1/1) with $NaBH_4$ (1.5 equiv) in 1,2-dichloroethane/EtOH (20/1, v/v) at 80 °C for 9 h and then washed with *n*-hexane. * denotes the ^{13}C satellite peaks of the solvent (b).

The ^{1}H NMR spectrum of the reaction products (Fig. S9e) was confirmed to be almost identical to those of the isolated *homo*-**DH3**$_{Na2}$ and *homo*-**DH4**$_{Na2}$ (Fig. S9c,d). The molar ratio of the products, *homo*-**DH3**$_{Na2}$: *homo*-**DH4**$_{Na2}$, was roughly estimated to be 39 : 61 from the ^{1}H NMR spectrum (Fig. S9e).

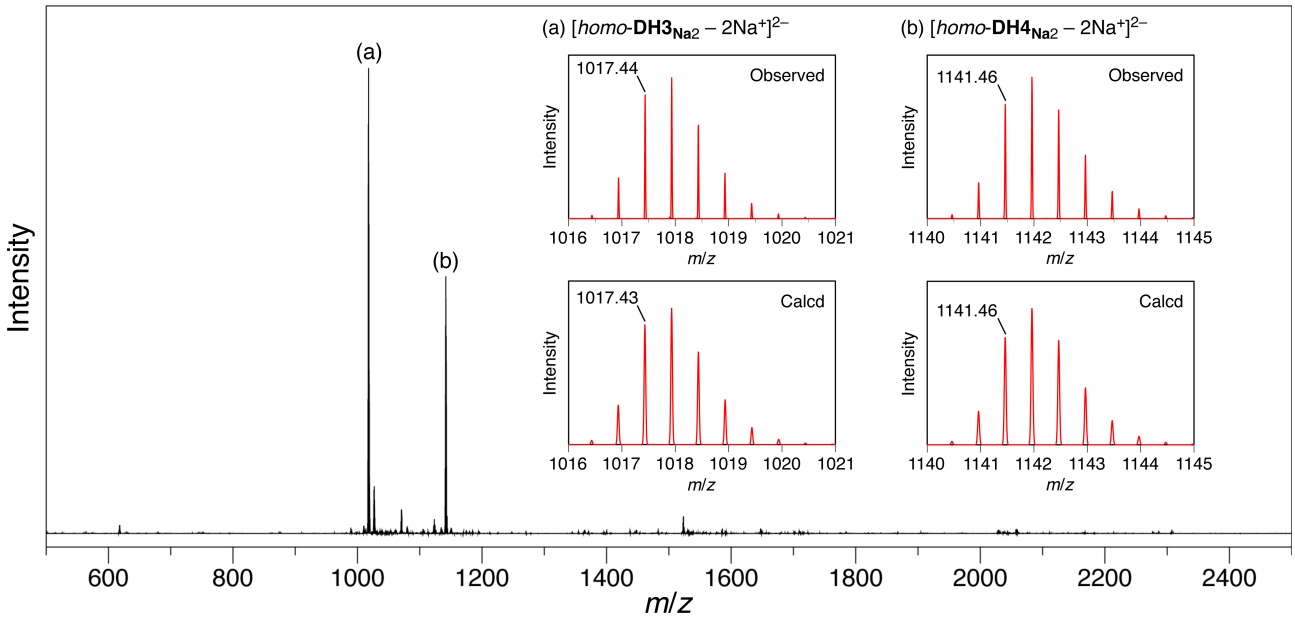

Fig. S10 Negative-mode ESI mass spectrum (CH_3CN/MeOH = 1/1, v/v) of the products after the reaction of **L3** and **L4** ([**L3**]/[**L4**] = 1/1) with $NaBH_4$ (1.5 equiv) in 1,2-dichloroethane/EtOH (20/1, v/v) at 80 °C for 9 h and then washed with *n*-hexane (Fig. S9e).

4. Theoretical Studies on the Structures of the *homo*- and *hetero*-Helicates.

The molecular modeling was performed on a Windows 7 PC with the ArgusLab software.[S2] The initial structures of the *homo*- and *hetero*-helicates were constructed based on the crystal structure of the left-handed double-stranded spiroborate helicate with a central porphyrin linker (*homo*-**DH2**$_{\mathbf{Na2}}$).[S1] One or two porphyrin units of the *homo*-**DH2**$^{2-}$ were replaced by the NDI and PDI residues to generate *homo*-**DH3**$^{2-}$, *homo*-**DH4**$^{2-}$, *hetero*-**DH2**·**3**$^{2-}$, *hetero*-**DH2**·**4**$^{2-}$ and *hetero*-**DH3**·**4**$^{2-}$. The linker units of all these initial structures were selectively geometry-optimized by molecular mechanics calculations (Universal force field (UFF)[S3] in ArgusLab software). The resulting structures were then fully optimized by the DFT calculations using the dispersion corrected B3LYP (B3LYP-D3)[S4] functional with the 6-31G* (for H, C, N, and O atoms) and the 6-31+G* (for B atoms) basis sets in *Gaussian 16* software.[S5] Computer resources for the DFT calculations were provided by the Information Technology Center of Nagoya University. The resultant energy-minimized structures are depicted in Figs. 3 and S11.

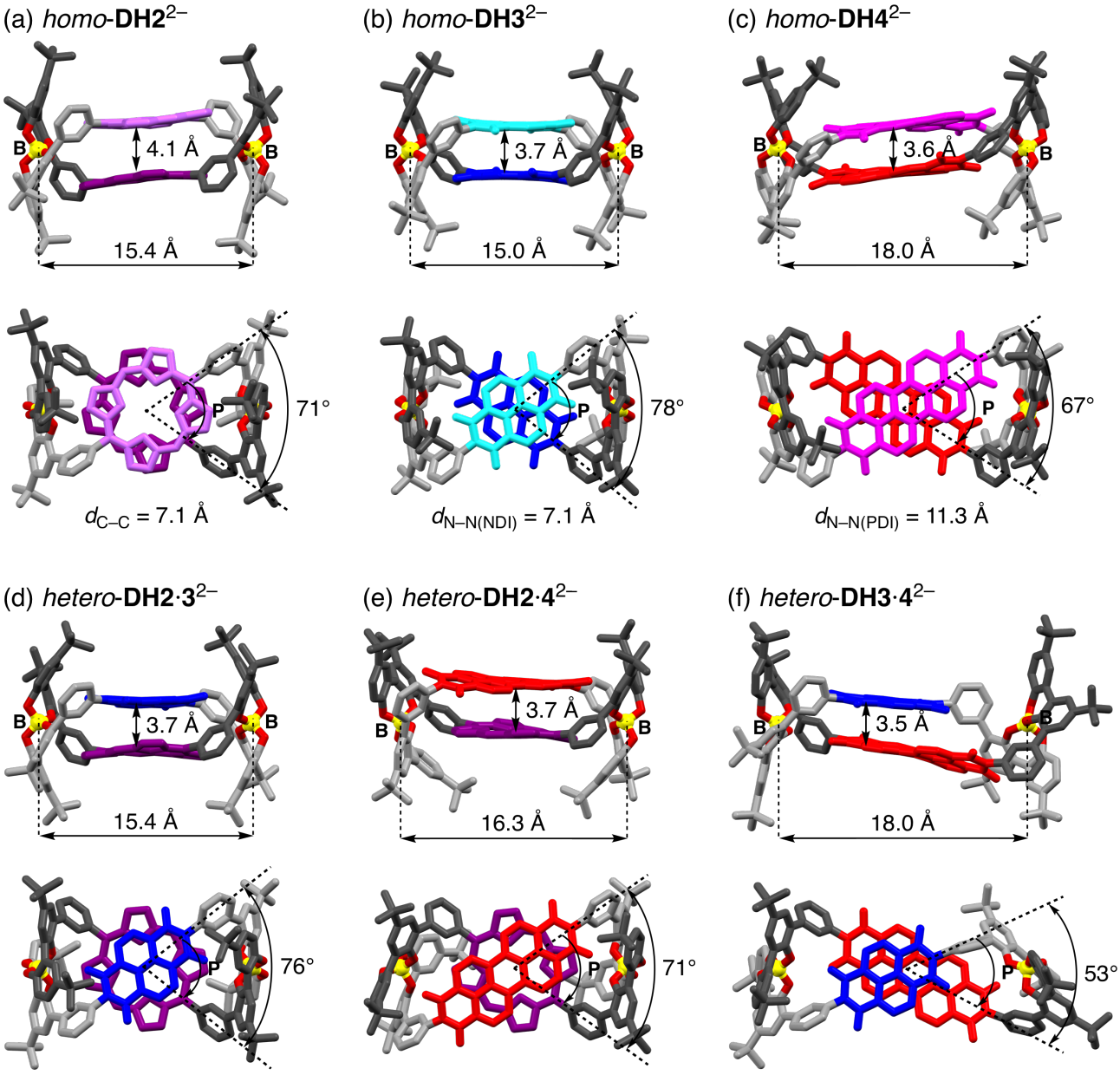

Fig. S11 The X-ray crystal structure of (a) left-handed *homo*-**DH2**$^{2-}$[S1] and the energy-minimized left-handed double-helical structures of (b) *homo*-**DH3**$^{2-}$, (c) *homo*-**DH4**$^{2-}$, (d) *hetero*-**DH2**·**3**$^{2-}$, (e) *hetero*-**DH2**·**4**$^{2-}$ and (f) *hetero*-**DH3**·**4**$^{2-}$ obtained by DFT calculations. All the hydrogen atoms are omitted for clarity.

5. 2D NMR Spectra of *homo*-DH3$_{Na2}$, *homo*-DH4$_{Na2}$ and *hetero*-DH2·3$_{Na2}$.

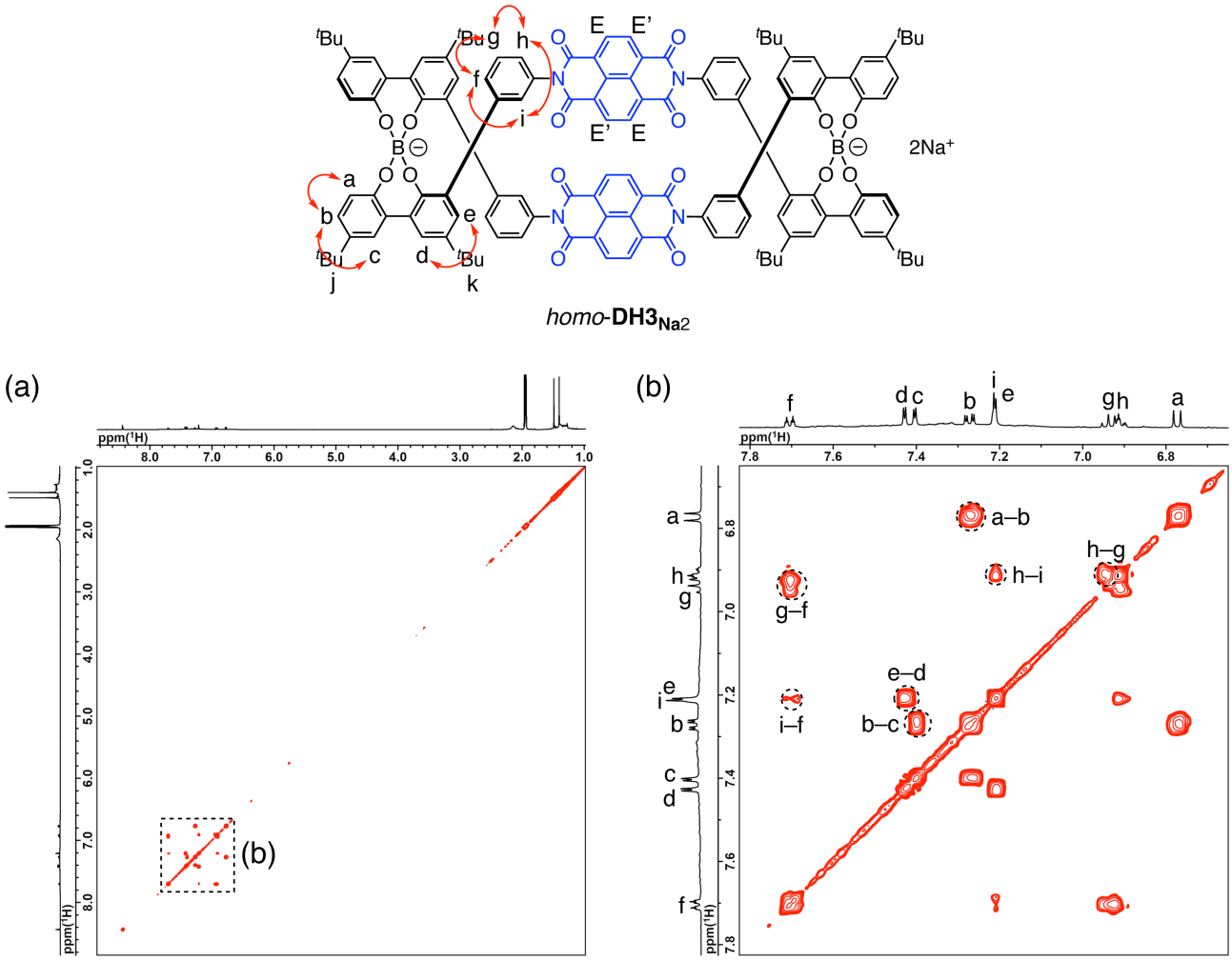

Fig. S12 (a) Full and (b) partial *g*COSY spectra of *homo*-DH3$_{Na2}$ (500 MHz, CD_3CN, 25 °C).

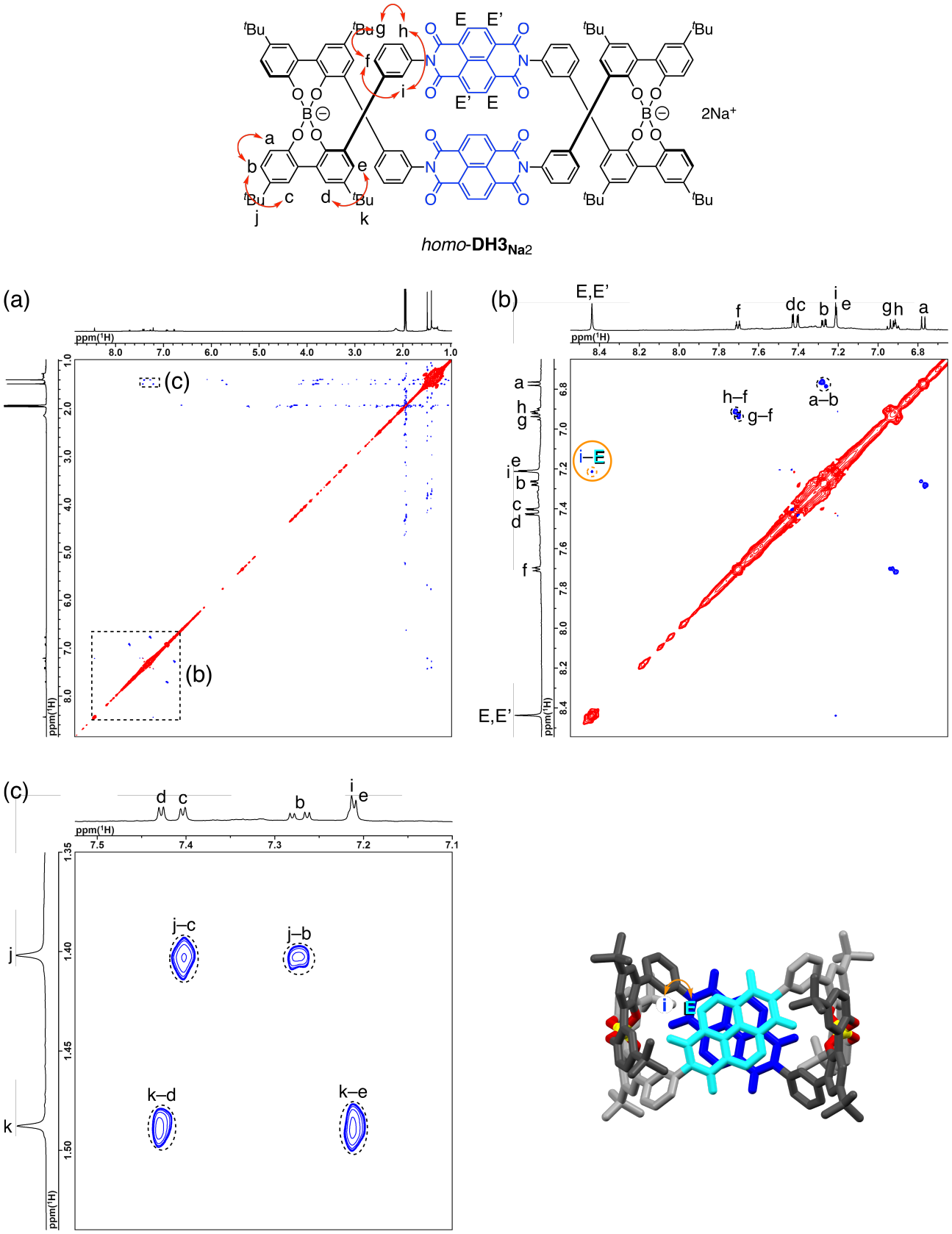

Fig. S13 (a) Full and (b,c) partial ROESY spectra of *homo*-**DH3**$_{Na2}$ (500 MHz, CD_3CN, 25 °C, mixing time = 200 ms).

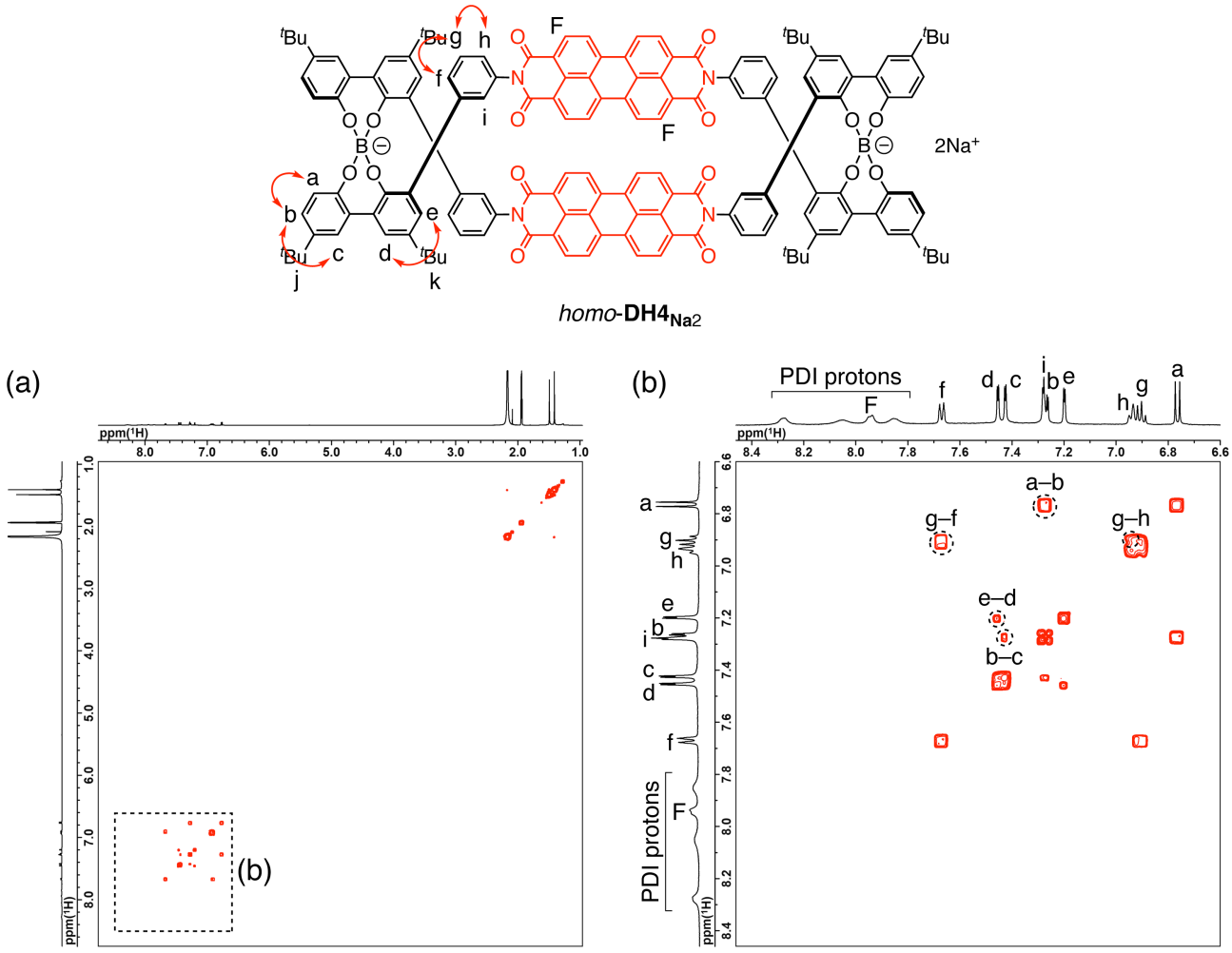

Fig. S14 (a) Full and (b) partial *g*COSY spectra of *homo*-**DH4**$_{Na2}$ (500 MHz, CD_3CN, 25 °C).

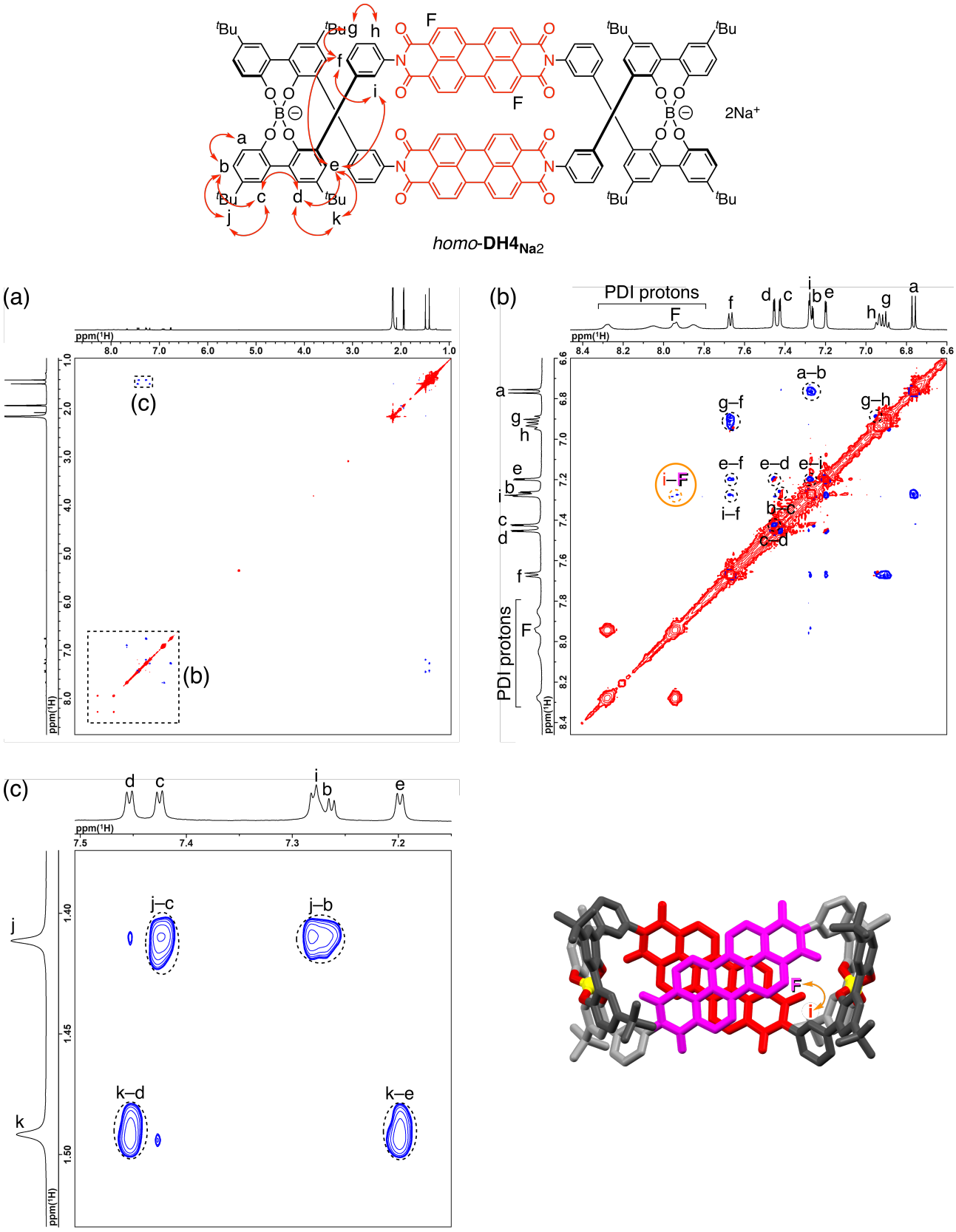

Fig. S15 (a) Full and (b,c) partial ROESY spectra of *homo*-**DH4**$_{Na2}$ (500 MHz, CD_3CN, 25 °C, mixing time = 200 ms).

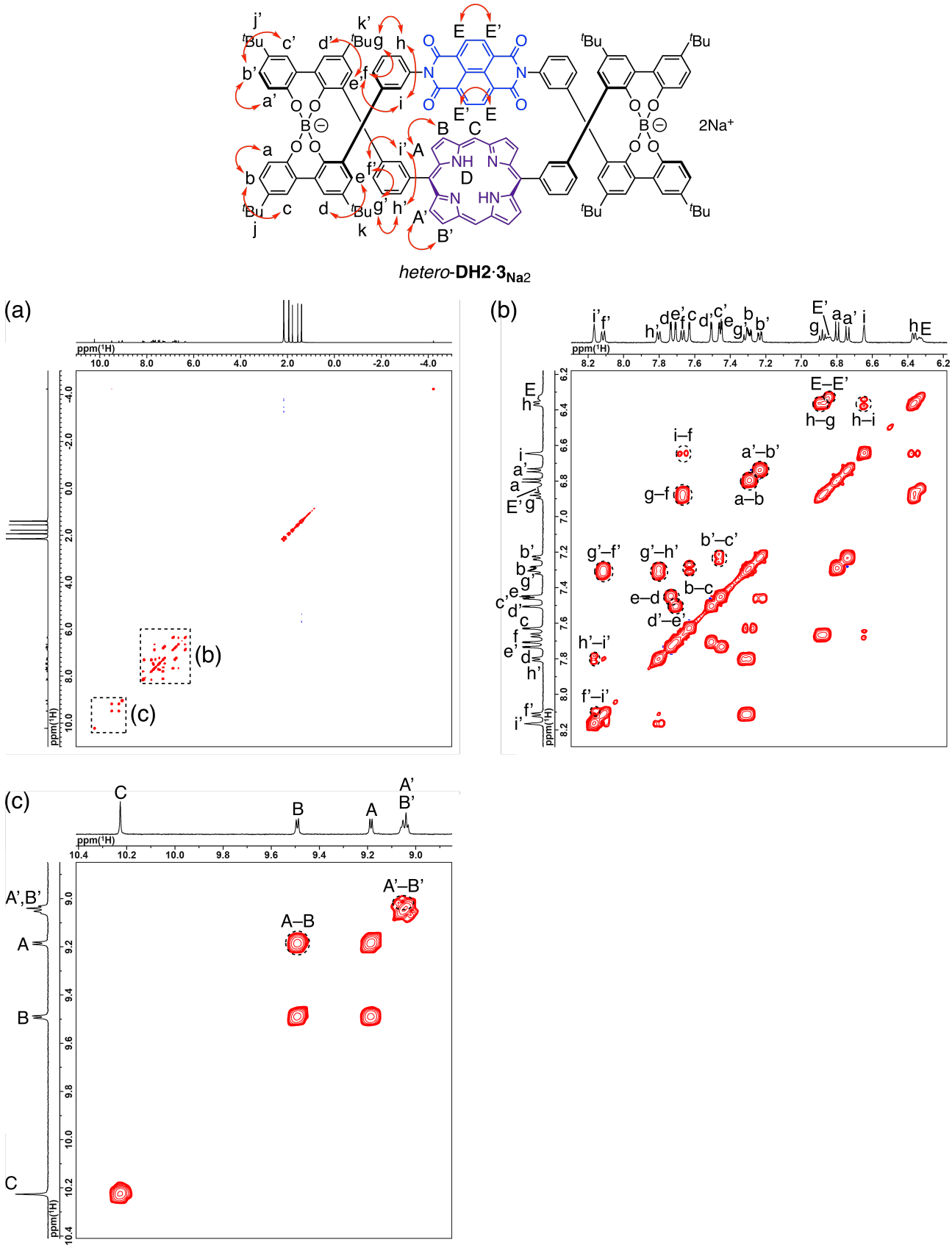

Fig. S16 (a) Full and (b,c) partial *g*COSY spectra of *hetero*-**DH2**·$\mathbf{3_{Na2}}$ (500 MHz, CD_3CN, 25 °C).

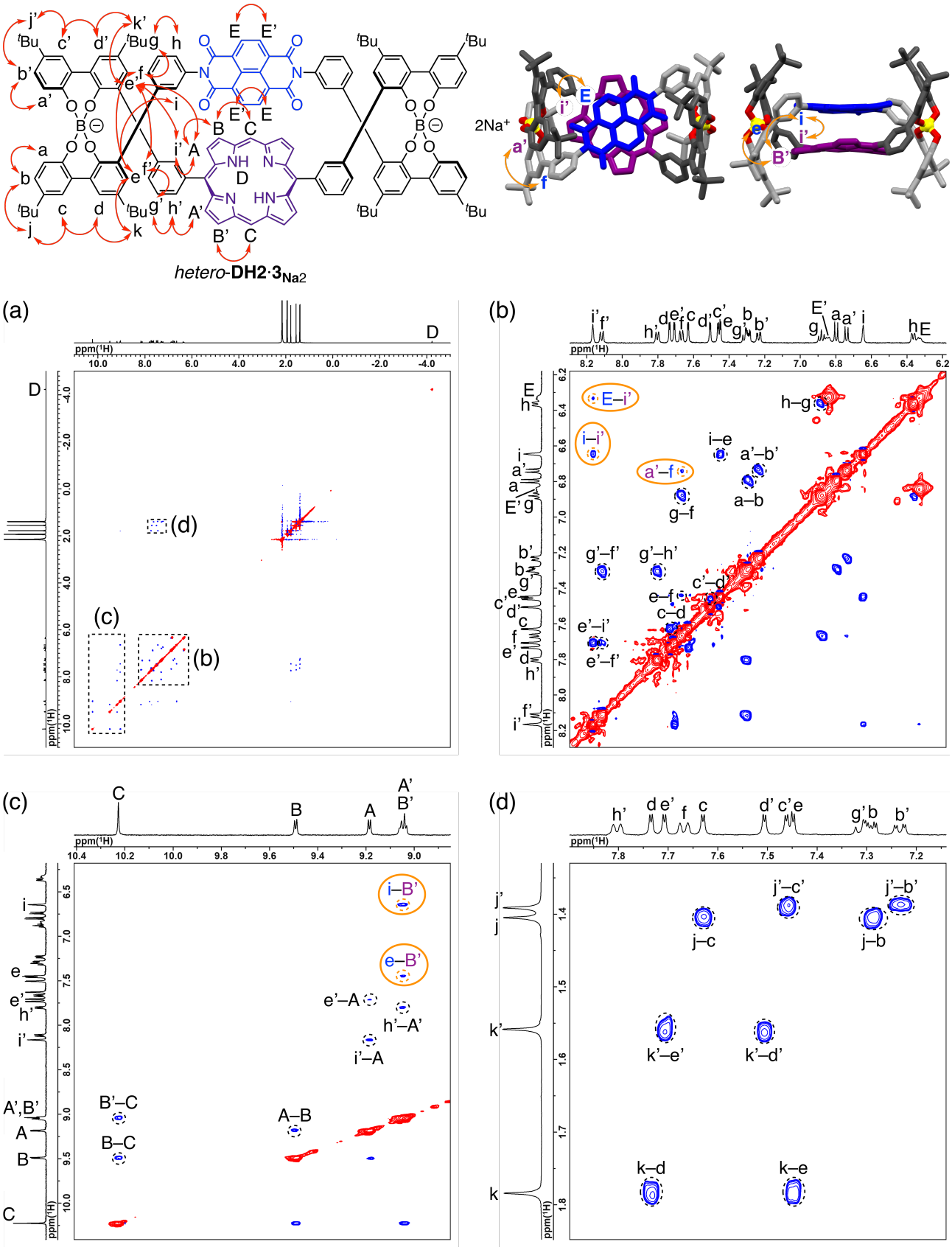

Fig. S17 (a) Full and (b–d) partial ROESY spectra of *hetero*-**DH2**·$\mathbf{3}_{Na2}$ (500 MHz, CD_3CN, 25 °C, mixing time = 200 ms).

6. Supporting References.

S1 S. Yamamoto, H. Iida and E. Yashima, *Angew. Chem., Int. Ed.*, 2013, **52**, 6849–6853.

S2 M. Thompson, ArgusLab, Planaria Software LLC, Seattle, WA (1996).

S3 A. K. Rappe, C. J. Casewit, K. S. Colwell, W. A. Goddard and W. M. Skiff, *J. Am. Chem. Soc.*, 1992, **114**, 10024–10035.

S4 S. Grimme, J. Antony, S. Ehrlich and H. Krieg, *J. Chem. Phys.*, 2010, **132**, 154104–154119.

S5 Gaussian 16, Revision A.03, M. J. Frisch, G. W. Trucks, H. B. Schlegel, G. E. Scuseria, M. A. Robb, J. R. Cheeseman, G. Scalmani, V. Barone, G. A. Petersson, H. Nakatsuji, X. Li, M. Caricato, A. V. Marenich, J. Bloino, B. G. Janesko, R. Gomperts, B. Mennucci, H. P. Hratchian, J. V. Ortiz, A. F. Izmaylov, J. L. Sonnenberg, D. Williams-Young, F. Ding, F. Lipparini, F. Egidi, J. Goings, B. Peng, A. Petrone, T. Henderson, D. Ranasinghe, V. G. Zakrzewski, J. Gao, N. Rega, G. Zheng, W. Liang, M. Hada, M. Ehara, K. Toyota, R. Fukuda, J. Hasegawa, M. Ishida, T. Nakajima, Y. Honda, O. Kitao, H. Nakai, T. Vreven, K. Throssell, J. A. Montgomery, Jr., J. E. Peralta, F. Ogliaro, M. J. Bearpark, J. J. Heyd, E. N. Brothers, K. N. Kudin, V. N. Staroverov, T. A. Keith, R. Kobayashi, J. Normand, K. Raghavachari, A. P. Rendell, J. C. Burant, S. S. Iyengar, J. Tomasi, M. Cossi, J. M. Millam, M. Klene, C. Adamo, R. Cammi, J. W. Ochterski, R. L. Martin, K. Morokuma, O. Farkas, J. B. Foresman and D. J. Fox, Gaussian, Inc., Wallingford CT, 2016.

7. Spectroscopic Data.

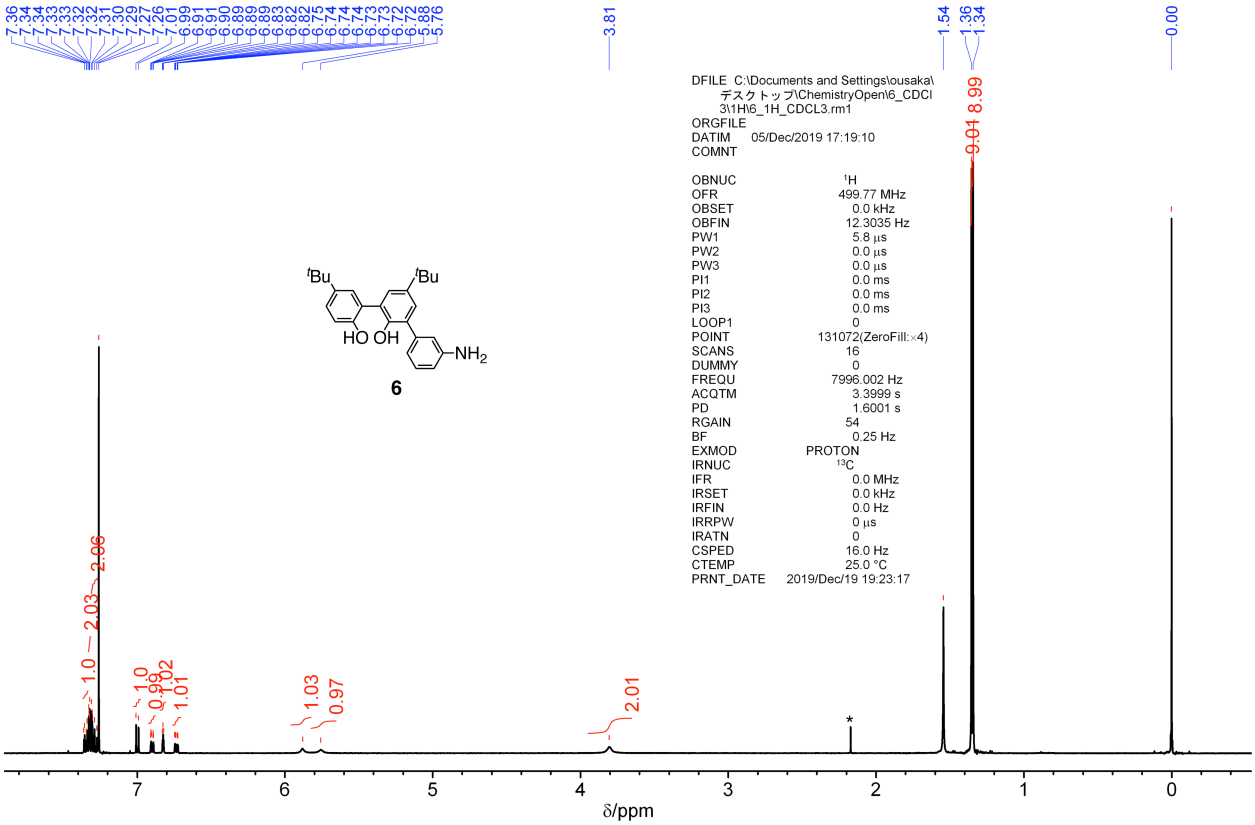

Fig. S18 ^{1}H NMR spectrum of **6** in $CDCl_3$ at 25 ºC. * denotes the proton from acetone.

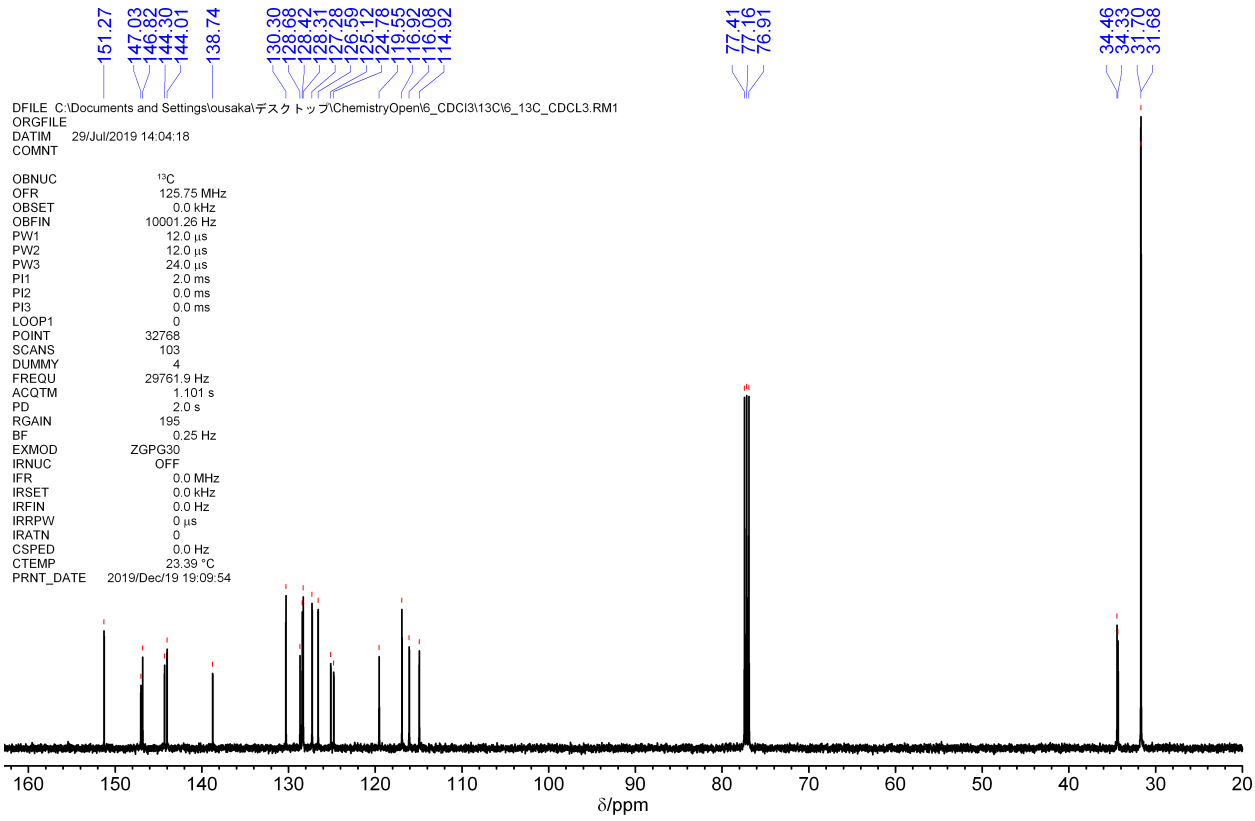

Fig. S19 ^{13}C NMR spectrum of **6** in $CDCl_3$ at 23 ºC.

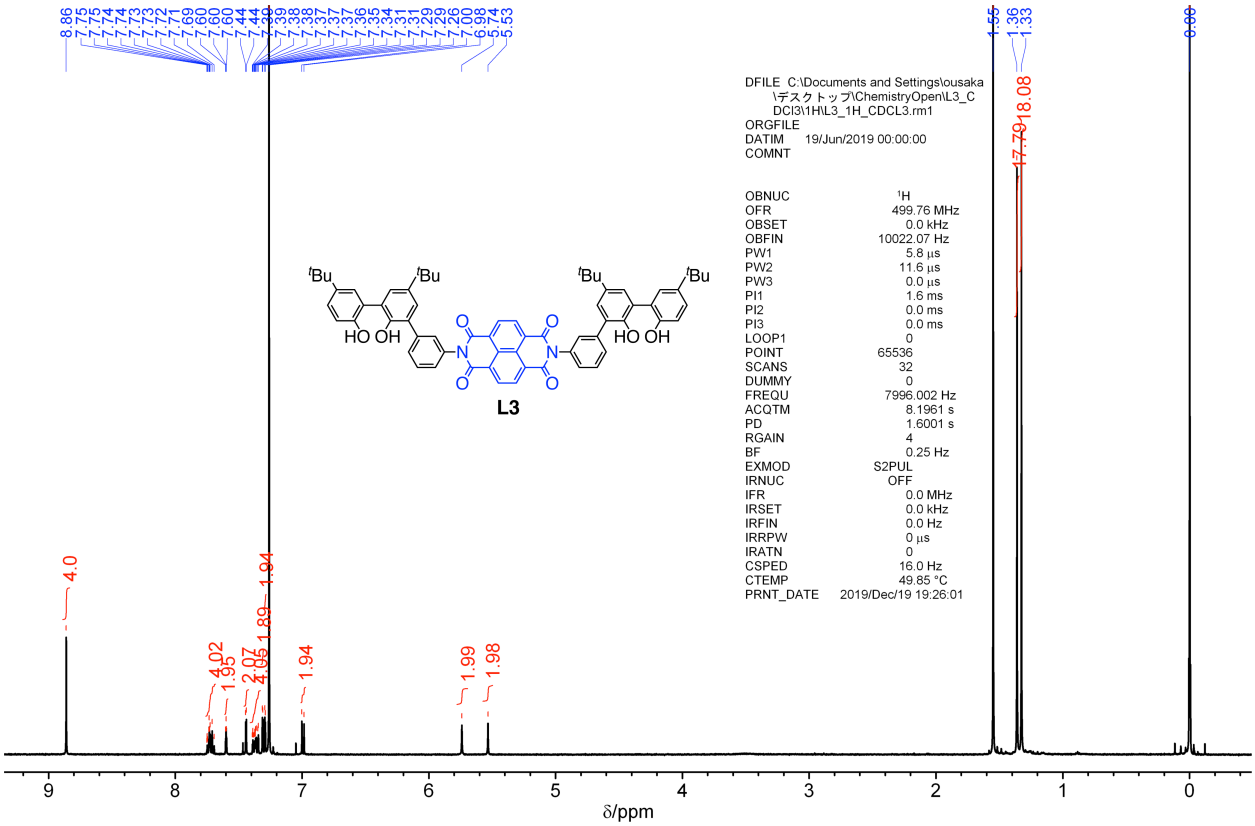

Fig. S20 ^{1}H NMR spectrum of **L3** in $CDCl_3$ at 50 ºC.

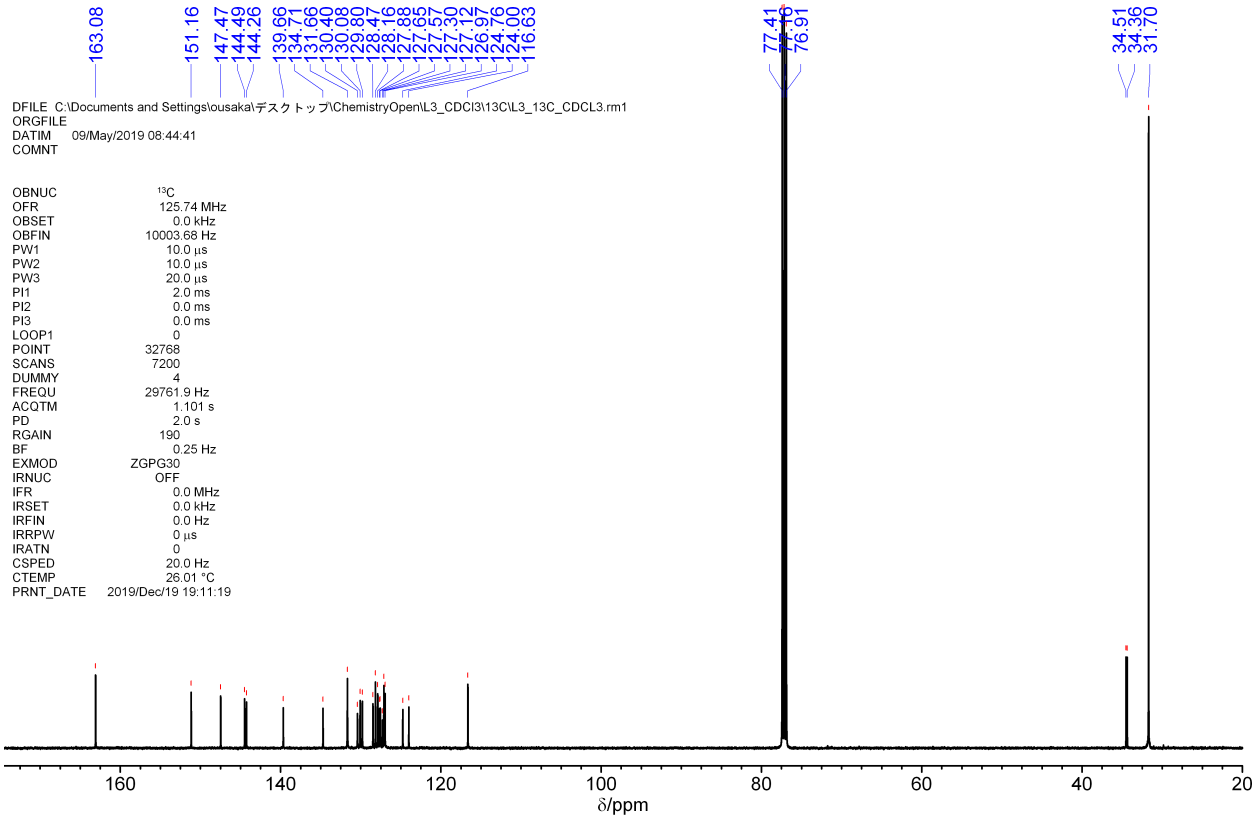

Fig. S21 ^{13}C NMR spectrum of **L3** in $CDCl_3$ at 26 ºC.

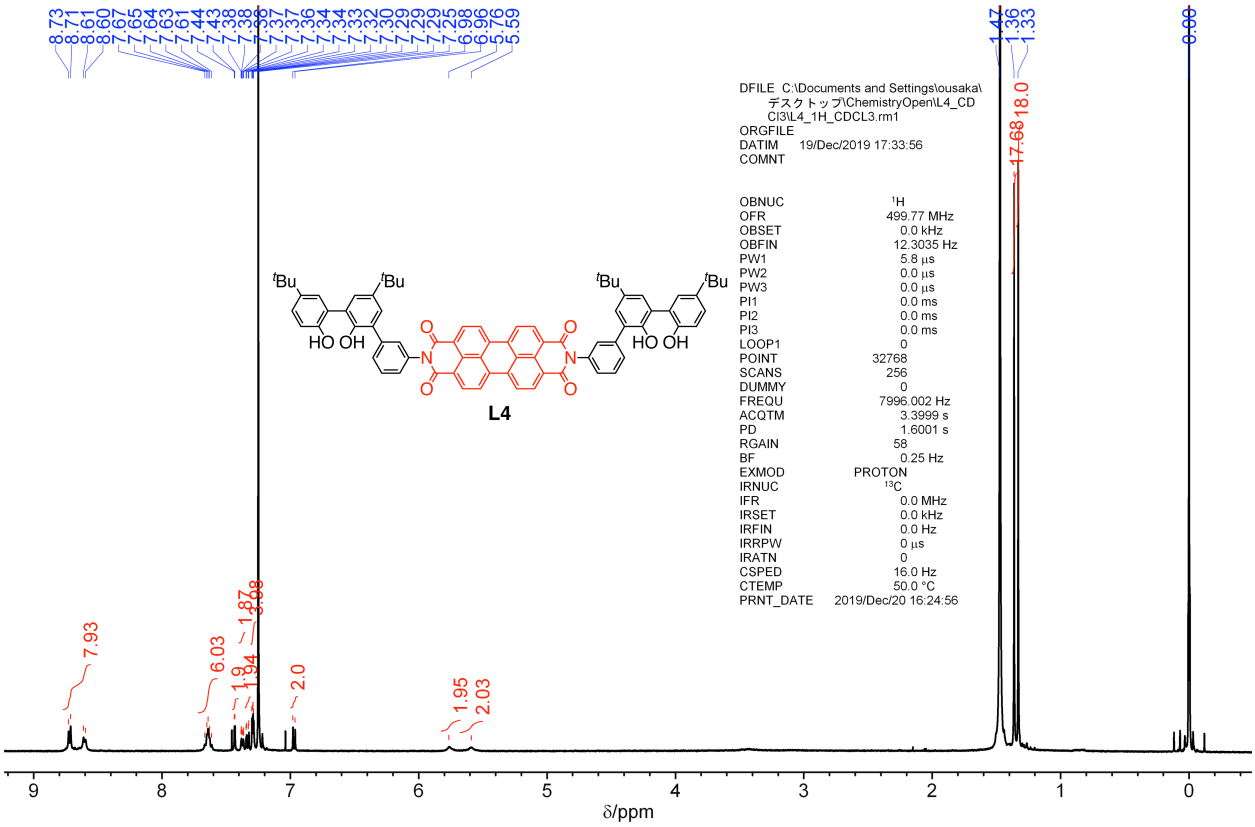

Fig. S22 ^{1}H NMR spectrum of **L4** in $CDCl_3$ at 50 ºC.

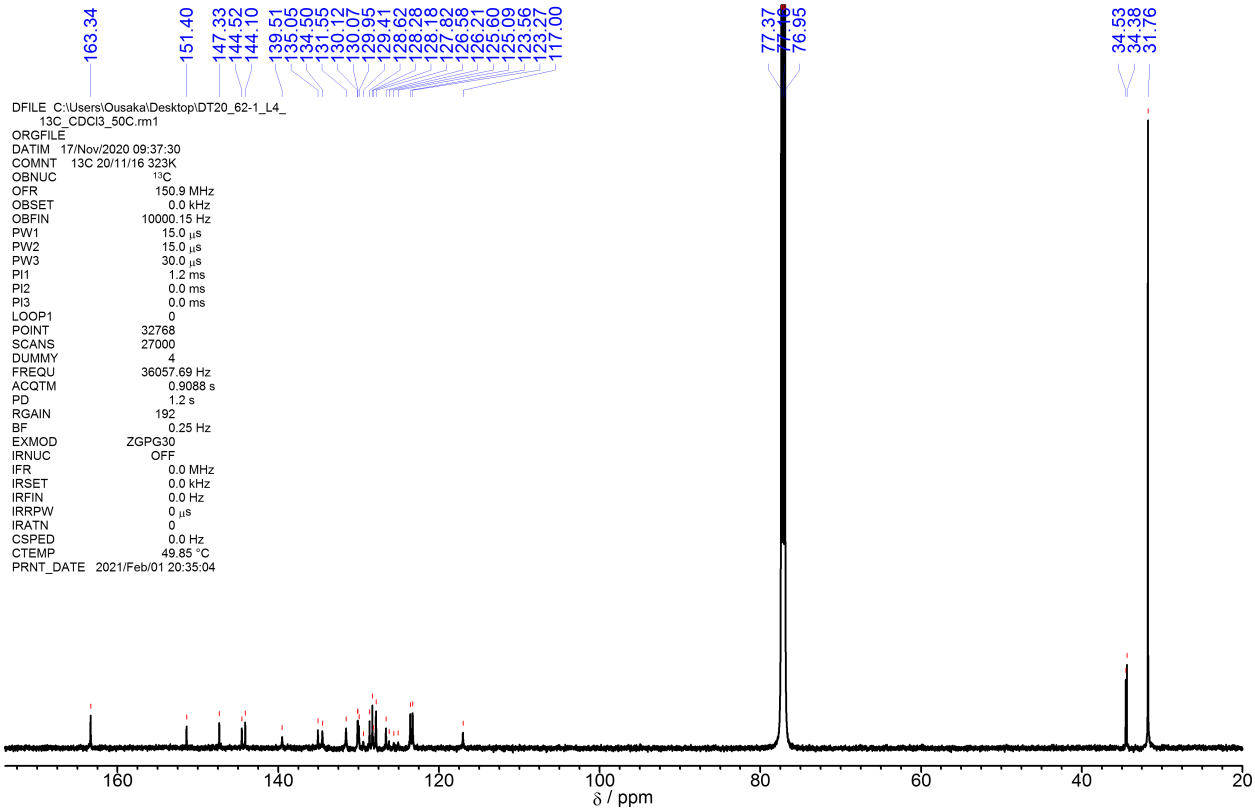

Fig. S23 ^{13}C NMR spectrum of **L4** in $CDCl_3$ at 50 ºC.

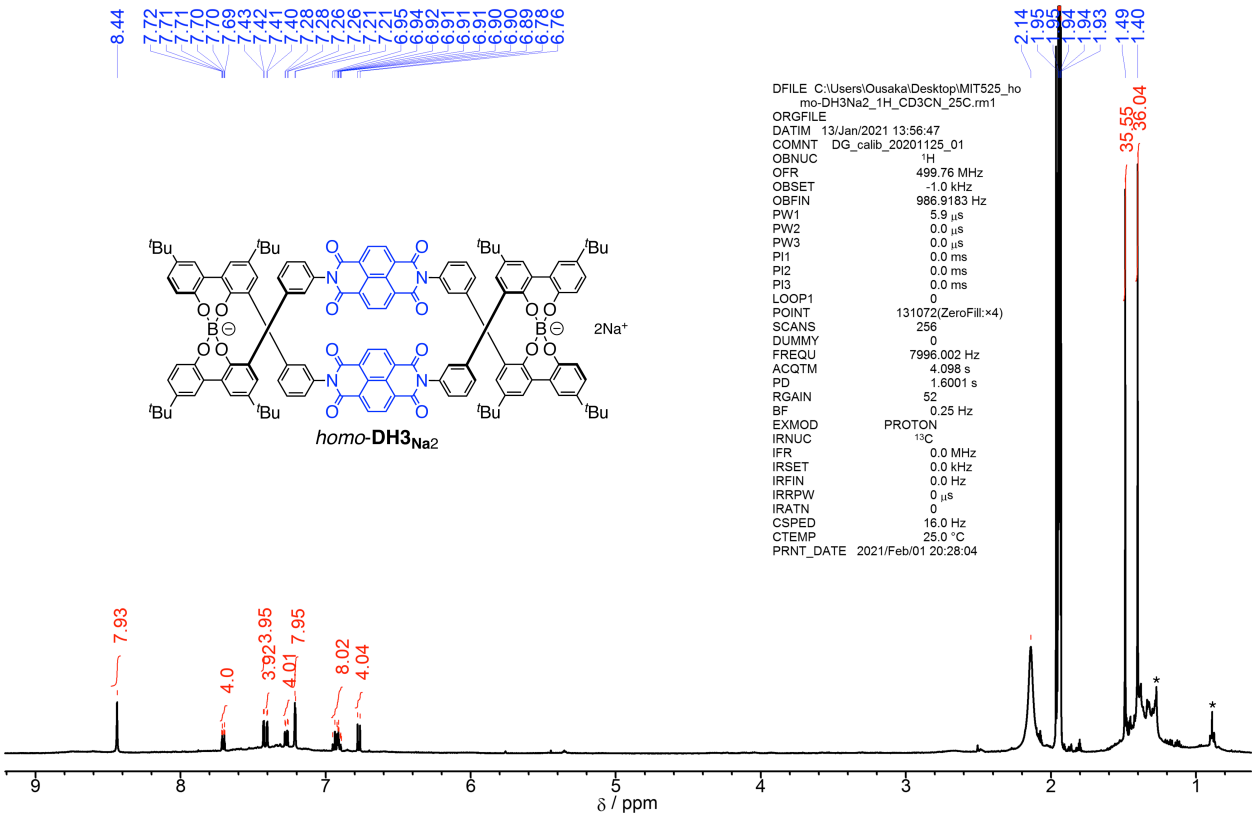

Fig. S24 ^{1}H NMR spectrum of *homo*-**DH3**$_{Na2}$ in CD_3CN at 25 ºC. * denote the protons from the residual *n*-hexane.

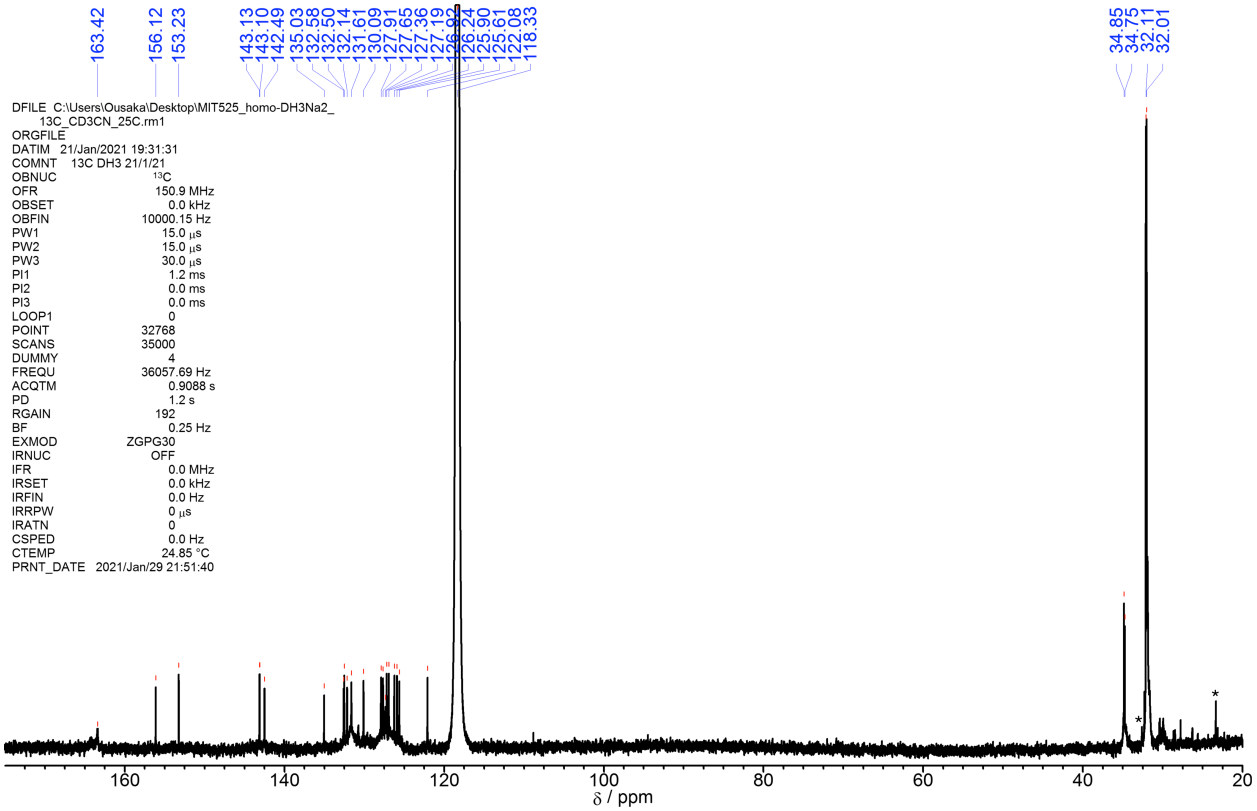

Fig. S25 ^{13}C NMR spectrum of *homo*-**DH3**$_{Na2}$ in CD_3CN at 25 ºC. * denote the carbons from the residual *n*-hexane.

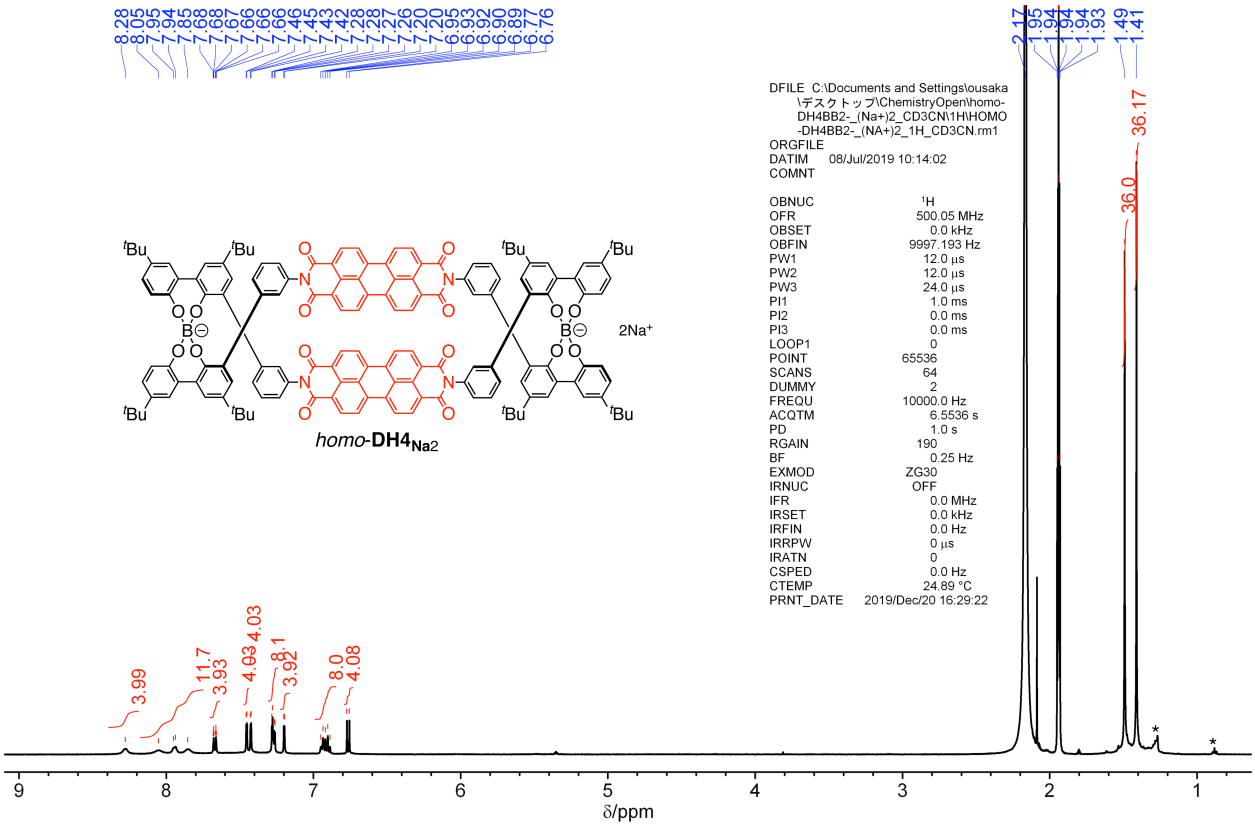

Fig. S26 ^{1}H NMR spectrum of *homo*-**DH4$_{Na2}$** in CD_3CN at 25 ºC. * denotes the protons from *n*-hexane.

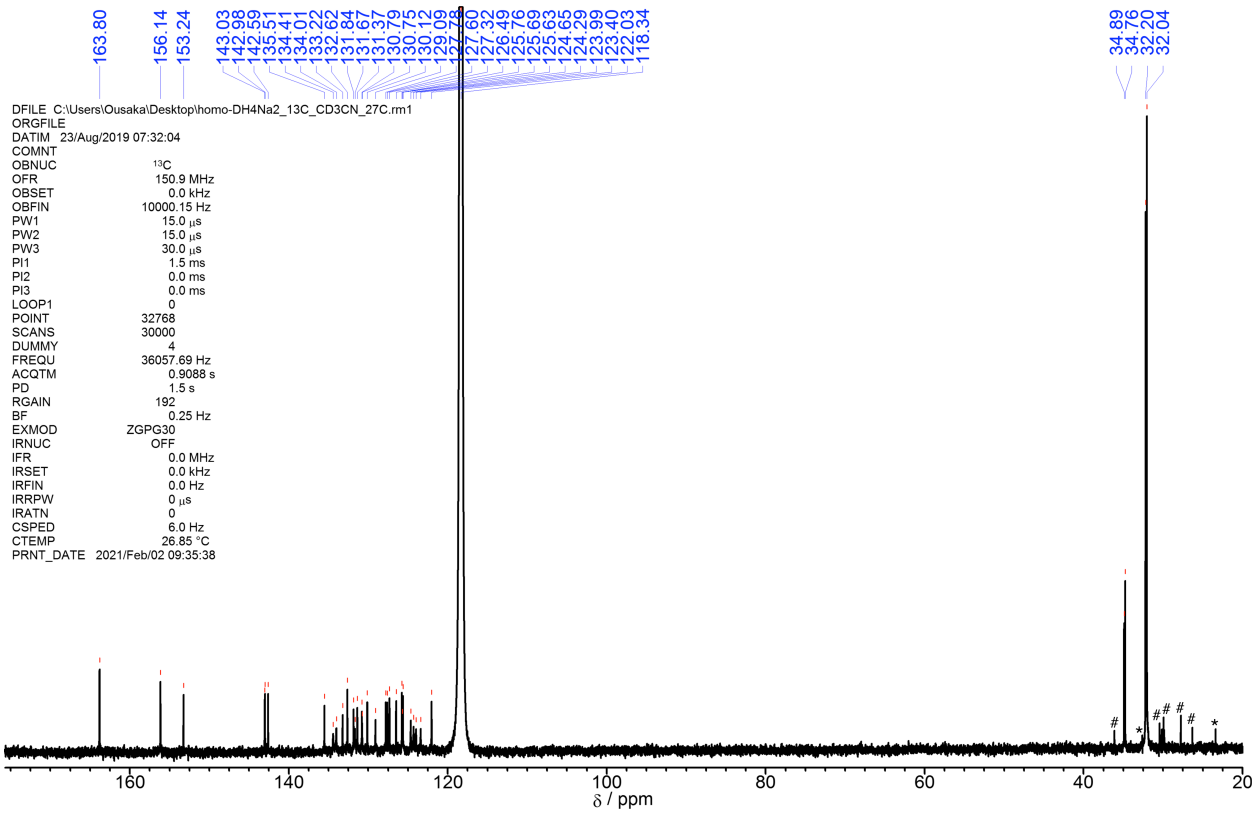

Fig. S27 ^{13}C NMR spectrum of *homo*-**DH4$_{Na2}$** in CD_3CN at 27 ºC. * and # denote the carbons from the residual *n*-hexane and the unknown impurities.

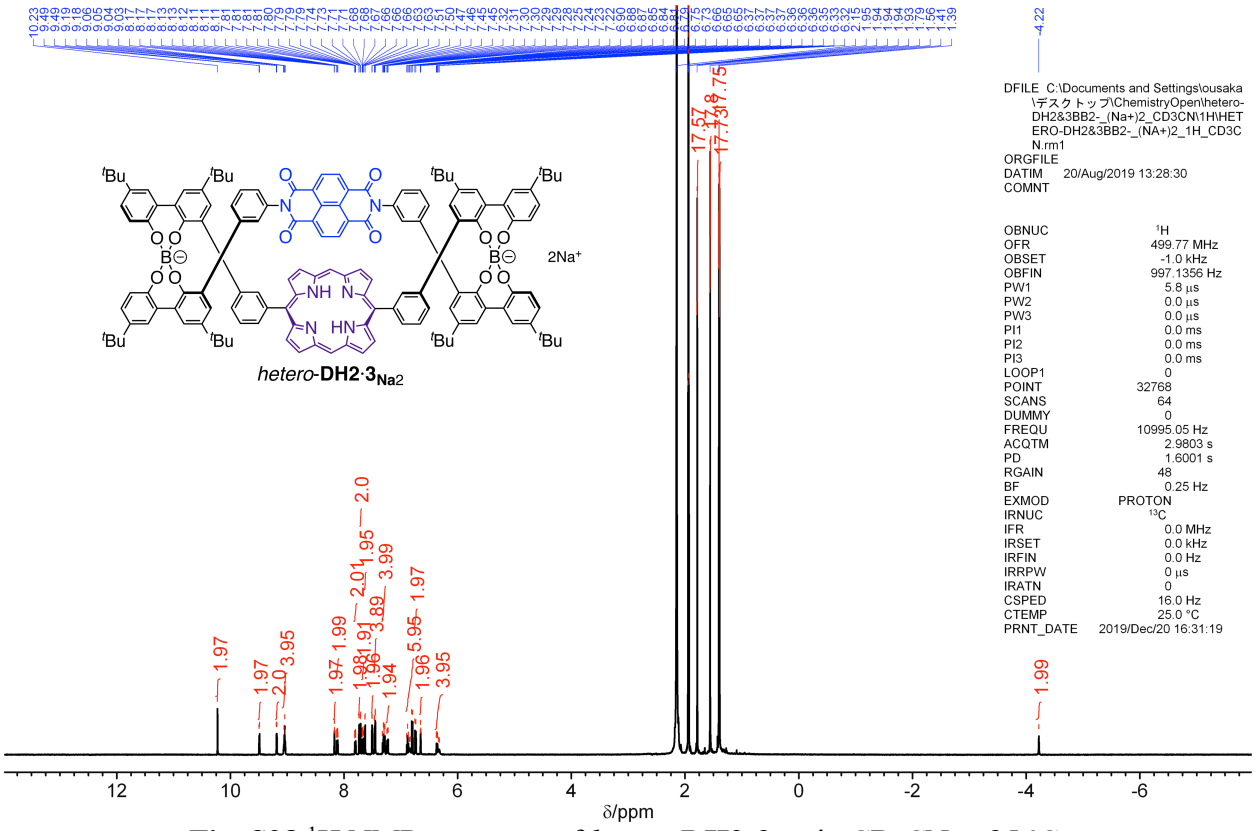

Fig. S28 ^{1}H NMR spectrum of *hetero*-**DH2·3$_{Na2}$** in CD_3CN at 25 ºC.

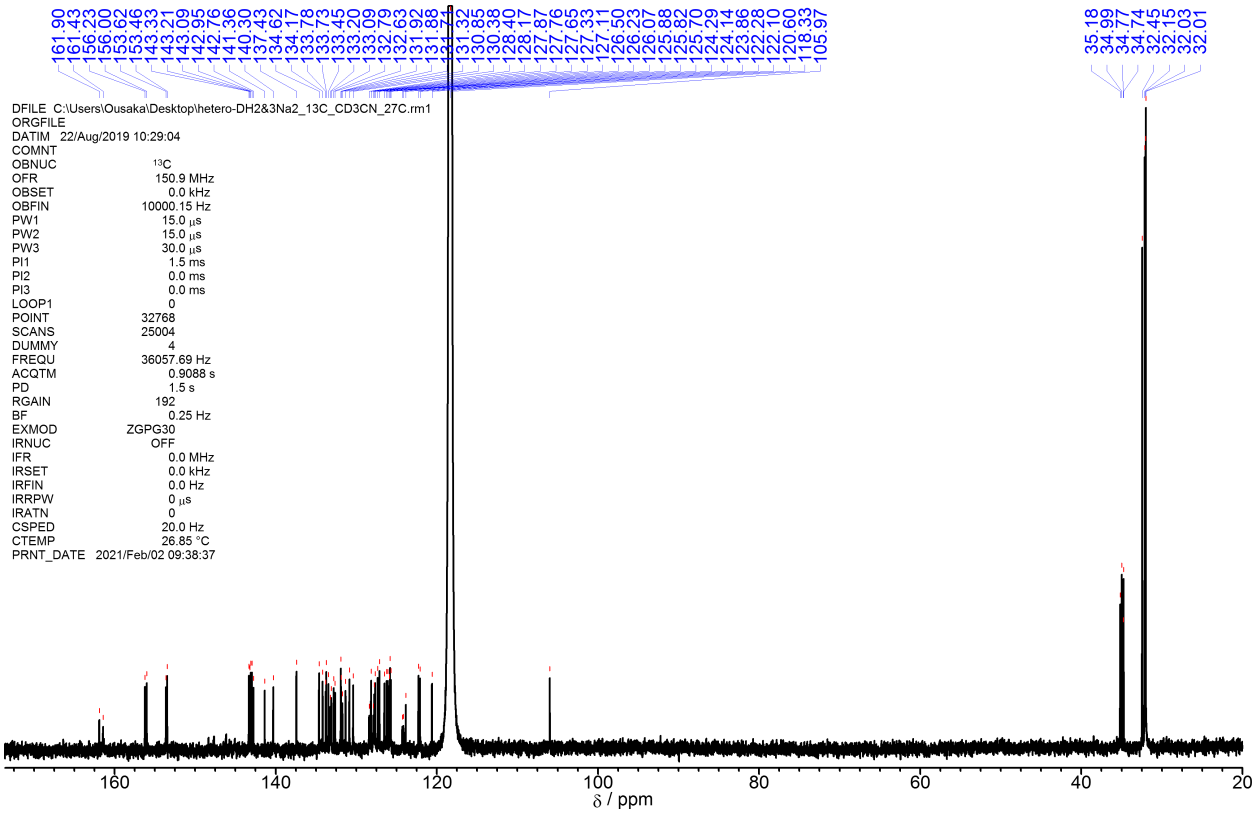

Fig. S29 ^{13}C NMR spectrum of *hetero*-**DH2·3$_{Na2}$** in CD_3CN at 27 ºC.